

Title Beta-cell specific insulin resistance promotes glucose-stimulated insulin hypersecretion

Authors Søs Skovsø¹, Evgeniy Panzhinskiy¹, Jelena Kolic¹, Derek A. Dionne¹, Xiao-Qing Dai², Rohit B. Sharma³, Lynda Elghazi⁴, Haoning Howard Cen¹, Cara E. Ellis¹, Katharine Faulkner⁵, Stephanie A.M. Marcil¹, Peter Overby¹, Nilou Noursadeghi¹, Daria Hutchinson¹, Xiaoke Hu¹, Hong Li¹, Honey Modi¹, Jen Wildi¹, J. Diego Botezelli¹, Hye Lim Noh⁶, Sujin Suk⁶, Brian Gablaski⁶, Austin Bautista², Ryekjang Kim², Corentin Cras-Méneur⁷, Stephane Flibotte⁸, Sunita Sinha⁹, Dan S. Luciani¹⁰, Corey Nislow⁹, Elizabeth J. Rideout¹, Eric N. Cytrynbaum⁵, Jason Kim^{6,12}, Ernesto Bernal-Mizrachi¹¹, Laura C. Alonso³, Patrick E. MacDonald², James D. Johnson¹

Affiliations

¹Diabetes Research Group, Life Sciences Institute, and Department of Cellular and Physiological Sciences, University of British Columbia, Vancouver, Canada

²Alberta Diabetes Institute and Department of Pharmacology, University of Alberta, Edmonton, Canada

³Division of Endocrinology, Diabetes and Metabolism, Weill Cornell Medicine, New York, USA

⁴Islet isolation Laboratory of the Animal Studies Core of the Michigan Diabetes Research Center, Department of Ophthalmology and Visual Sciences, University of Michigan Kellogg Eye Center, Ann Arbor, MI, USA

⁵Department of Mathematics, University of British Columbia, Vancouver, Canada

⁶Program in Molecular Medicine University of Massachusetts Medical School, USA

⁷Department of Internal Medicine, Division of Metabolism, Endocrinology and Diabetes, University of Michigan, Ann Arbor, MI USA

⁸UBC Life Sciences Institute Bioinformatics Facility, University of British Columbia, Vancouver, Canada

⁹UBC Sequencing and Bioinformatics Consortium, Pharmaceutical Sciences, University of British Columbia, Vancouver, Canada

¹⁰BC Children's Hospital Research Institute, Department of Surgery, Faculty of Medicine, University of British Columbia, Vancouver, Canada

¹¹Division of Endocrinology, Diabetes and Metabolism, University of Miami Miller School of Medicine, Miami, USA

¹²Division of Endocrinology, Metabolism, and Diabetes, Department of Medicine, University of Massachusetts Medical School, USA

Address correspondence to James D. Johnson, PhD., Faculty of Medicine, Department Cellular and Physiological Sciences, The University of British Columbia, Life Sciences Institute, 5358 – 2350 Health Sciences Mall, Vancouver, British Columbia, Canada V6T 1Z3 Email James.d.johnson@ubc.ca, Twitter @JimJohnsonSci

Abstract Word Count 289

Body Word Count 10176

Reference Count 102

Figure Count 7

Supplemental Figure Count 10

Data availability Raw RNAseq data are deposited in GEO.

Author contributions

S.S. led project design/management, conducted experiments, analyzed data, and wrote the manuscript.
E. P. conducted experiments, analyzed data, and edited the manuscript (protein synthesis, Westerns).
J. K. conducted experiments, analyzed data, and edited the manuscript (ex vivo insulin secretion).
D. A. D. conducted experiments and analyzed data (in vivo glucose homeostasis).
X-Q. D. conducted experiments, analyzed data, and edited the manuscript (electrophysiology).
R. B. S. conducted experiments, analyzed data, and edited the manuscript (long-term hyperglycemia, proliferation).
L. E. conducted experiments, analyzed data, and edited the manuscript (MIP^{Cre} mice)
H. H. C. analyzed data, and edited the manuscript (RNAseq analysis)
C. E. analyzed data, and edited the manuscript (Bioinformatics and calcium data analysis)
K. F. analyzed data, and edited the manuscript (mathematical modelling)
S. A. M. M. conducted experiments and analyzed data (beta-cell area)
N. N. conducted experiments (imaging)
P. O. conducted experiments, analyzed data, and edited the manuscript (Seahorse)
D. H. conducted experiments (mRNA expression qPCR)
X. H. conducted experiments (in vivo physiology)
H. L. conducted experiments (in vivo physiology)
H. M. conducted experiments, analyzed data, and edited the manuscript (FACS, RNAseq prep)
J. W. conducted experiments (beta cell insr western blots)
J. D. B. conducted experiments (liver insr western blots)
H. L. N. conducted experiments (hyperglycemic clamps)
S. S. conducted experiments (hyperglycemic clamps)
A.B. conducted experiments (electrophysiology).
R.K. conducted experiments (electrophysiology).
B. G. conducted experiments (long-term hyperglycemia, proliferation).
C. C-M. conducted experiments, and edited the manuscript (MIP^{Cre} mice)
S. F. analyzed data (RNAseq analysis)
S. S. conducted experiments (RNAseq)
D. S. L. conducted experiments and edited the manuscript (nTnG validation)
C. N. supervised experiments, and edited the manuscript (RNAseq)
E.J.R supervised experiments, and edited the manuscript
E.N.C. supervised experiments, and edited the manuscript (mathematical modeling)
J. K. supervised studies, and edited the manuscript (Hyperglycemic clamps)
E. B-M. supervised studies, and edited the manuscript (MIP^{Cre} mice)
L. A. supervised studies, and edited the manuscript (long-term hyperglycemia, proliferation)
P. E. M. supervised studies, and edited the manuscript (electrophysiology)
J. D. J. conceived the project, oversaw its execution, edited the manuscript, and guarantees the work.

Acknowledgements

We thank Johnson lab members for valuable feedback and those who provided insight when data was presented at conferences. We also thank Sarah Hulme, Charles Nieh and our animal care staff for supporting our animal husbandry, Bernard Thorens and Jorge Ferrer for sharing the $Ins1^{cre}$ knock-in mice, Eric Jan for allowing us to use his facilities to conduct S^{35} labeling. We thank Quin Wills for helpful discussion of the smartseq2 protocol, and Austin Taylor for discussion of genotyping.

Funding

SS was supported by an Alfred Benzon Post-Doctoral fellowship. Work was primarily supported by a CIHR grant (133692) to JDJ. Work in Edmonton was supported by CIHR grant (148451) to PEM. Work in the Michigan Diabetes Research Center was supported by NIH (P30 DK020572). Work at U Mass was supported by an NIH grants (5U2C-DK093000) to JKK and (R01DK114686) to LCA. CN is supported as a Tier 1 CRC.

Conflict of Interest Statement

The authors report no conflicts of interest related to this work.

Abstract

Insulin receptor (*Insr*) protein can be found at higher levels in pancreatic β -cells than in most other cell types, but the consequences of β -cell insulin resistance remain enigmatic. *Ins1^{cre}* allele was used to delete *Insr* specifically in β -cells of both female and male mice which were compared to *Ins1^{cre}*-containing littermate controls at multiple ages and on multiple diets. RNA-seq of recombined β -cells revealed significant differences in multiple pathways previously implicated in insulin secretion and cellular fate, including rewired Ras and NF κ B signaling. Male, but not female, β /*Insr*^{KO} mice had reduced oxygen consumption rate, while action potential and calcium oscillation frequencies were increased in *Insr* knockout β -cells from female, but not male mice. Female β /*Insr*^{KO} and β /*Insr*^{HET} mice exhibited elevated insulin release in perfusion experiments, during hyperglycemic clamps, and following *i.p.* glucose challenge. Deletion of *Insr* did not reduce β -cell mass up to 9 months of age, nor did it impair hyperglycemia-induced proliferation. Based on our data, we adapted a mathematical model to include β -cell insulin resistance, which predicted that β -cell *Insr* knockout would improve glucose tolerance depending on the degree of whole-body insulin resistance. Indeed, glucose tolerance was significantly improved in female β /*Insr*^{KO} and β /*Insr*^{HET} mice when compared to controls at 9, 21 and 39 weeks. We did not observe improved glucose tolerance in adult male mice or in high fat diet-fed mice, corroborating the prediction that global insulin resistance obscures the effects of β -cell specific insulin resistance. We further validated our *in vivo* findings using the *Ins1-CreERT* transgenic line and found improved glucose tolerance 4 weeks after tamoxifen-mediated *Insr* deletion. Collectively, our data show that loss of β -cell *Insr* alone is sufficient to drive glucose-induced hyperinsulinemia, thereby improving glucose homeostasis in otherwise insulin sensitive dietary and age contexts.

Introduction

Type 2 diabetes is a multifactorial disease wherein several cell types, most prominently pancreatic β -cells, are dysfunctional prior to and after diagnosis (Prentki and Nolan, 2006). Hyperinsulinemia, insulin resistance, impaired fasting glucose, and impaired glucose tolerance can all be observed prior to the onset of frank diabetes (Tabak et al., 2012), but the causal relationships between these factors remain incompletely understood (Page and Johnson, 2018). Impaired insulin receptor signaling is associated with obesity and often precedes the onset of overt type 2 diabetes, but it has been studied primarily in skeletal muscle, fat, and liver where it manifests differently (Boucher et al., 2014). Recent work in mice has established that β -cell specific insulin resistance can be observed early in the progression towards type 2 diabetes, when hyperinsulinemia is prominent, and independently of insulin resistance in other tissues (Paschen et al., 2019). The physiological consequences of reduced insulin receptor (*Insr*)-mediated signaling in β -cells remain controversial.

It remains unresolved whether physiological insulin action on β -cells manifests as positive feedback to stimulate further insulin secretion, or negative feedback to inhibit its own release (Leibiger et al., 2008). Human studies provide evidence for both possibilities. *In vivo* hyperinsulinemic-euglycemic clamps have been shown to reduce circulating C-peptide, a marker of endogenous insulin secretion (Cavallo-Perin et al., 1993; Elahi et al., 1982). In some studies, this inhibition was impaired in the obese state suggesting that systemic insulin resistance also extends to the β -cells (Cavallo-Perin et al., 1993). Bouche and colleagues replicated this result at basal glucose, but also found evidence that insulin can potentiate glucose-stimulated insulin secretion under specific conditions (Bouche et al., 2010). Others have shown that insulin can either stimulate or inhibit its own secretion depending on the metabolic context (Mari et al., 2011). Administration of insulin to single β -cells *in vitro* increases intracellular Ca²⁺ (Johnson and Misler, 2002a) and, in some studies, stimulates exocytosis (Aspinwall et al., 1999). However, Ca²⁺ release from intracellular stores is not always sufficient to evoke insulin exocytosis. We previously did not detect robust exocytosis or C-peptide release from human β -cells in response to exogenous insulin despite observed changes in Ca²⁺ release (Luciani and Johnson, 2005).

Whether chronic changes in autocrine insulin signaling affect β -cell development, survival and adaptation conditions is also controversial. Mice with chronically reduced insulin production have

impaired β -cell expansion in the context of a high fat diet (Mehran et al., 2012). *In vitro*, physiologically relevant concentrations of insulin support the survival of both human and mouse β -cells (Johnson et al., 2006a). We also reported insulin is sufficient to increase proliferation of cultured primary mouse β -cells and that blocking insulin secretion with somatostatin blunts proliferation induced by hyperglycemia *in vitro* (Beith et al., 2008) and that the majority of glucose-dependent changes in gene expression in MIN6 cells are *Insr*-dependent (Ohsugi et al., 2005). However, it has also been proposed hyperglycemia-induced β -cell proliferation bypasses the *Insr* (Jhala et al., 2003; Stamateris et al., 2016). Thus, whether these signals from insulin and/or glucose are transmitted through *Insr*, *Igf1r*, or both receptors, remains unresolved.

To address the short- and long-term consequences of eliminating *Insr* signaling *in vivo*, Kulkarni and colleagues generated mice with a floxed *Insr* allele and an *Ins2* promoter driven Cre transgene (Kulkarni et al., 1999). Using this and related models, they reported that mice lacking β -cell *Insr* have profound glucose intolerance, and frank diabetes in some cases, due to impaired glucose stimulated insulin secretion, Glut2 loss, and insufficient β -cell mass (Kulkarni et al., 1999; Okada et al., 2007; Otani et al., 2004). Mice lacking *Insr* in β -cells (and other off-target cell types) failed to exhibit the compensatory increase in β -cell mass that accompanies a high fat diet in mice (Okada et al., 2007). Doubt was cast on some of these results when these Cre lines were subsequently shown to have off-target tissue effects owing to endogenous *Ins2* expression in the brain and thymus (Fan et al., 2009; Johnson, 2014; Mehran et al., 2012; Wicksteed et al., 2010a). More recently, Wang and colleagues studied the roles of β -cell *Insr* *in utero* and in adult mice using an inducible *Ins1*-CreER transgenic mouse model (Oakie et al., 2020; Wang et al., 2018), but these studies are confounded by the presence of the human growth hormone (hGH) minigene (Oropeza et al., 2015), which necessitates the use of Cre-containing controls exclusively.

In the present study, we used the constitutive *Ins1*^{Cre} knock-in strain with robust and specific recombination in β -cells (Thorens et al., 2015) to precisely reduce insulin receptor signaling and define the impacts of β -cell specific insulin resistance on glucose homeostasis. Using this approach, we found that insulin receptor signaling plays a suppressive role on insulin secretion by modulating β -cell electrical excitability and that this effect is absent in conditions of global insulin resistance.

Results

Insr abundance in human islets and β -cells

We initiated our studies by conducting an unbiased analysis of insulin receptor abundance across tissues using publicly accessible data. Pancreatic islets had the 2nd highest protein abundance of both isoforms of the insulin receptor across a panel of 24 human tissues, as quantified by mass-spectrometry (Fig. 1A). These results, which are not complicated by the limitations associated with anti-*insr* antibodies, show that islets have more INSR protein than ‘classical’ insulin target tissues, including the liver and adipose. This also supports our previous observations suggesting that insulin receptors are more abundant in β -cells relative to other cells in the pancreas (Boothe et al., 2016). Compilation of open source public single-cell RNA sequencing data from human islets demonstrated at least one count of insulin receptor mRNA in 62.4% β -cells, alongside other islet cell types (Fig. 1A,B).

β -cell specific *Insr* deletion with *Ins1*^{Cre} mice

We next sought to examine the function of the *Insr*, and the consequences of β -cell-specific insulin resistance/sensitivity, using an *in vivo* β -cell specific knockout mouse model. To limit recombination of the floxed *Insr* allele to pancreatic β -cells, we used a Cre allele knocked into the endogenous *Ins1* locus which, unlike *Ins2* promoters, drives specific expression in β -cells (Thorens et al., 2015). Experimental *Insr*^{f/f},*Ins1*^{cre/wt},nTnG (β /*Insr*^{KO}) and *Insr*^{f/wt},*Ins1*^{cre/wt},nTnG (β /*Insr*^{HET}) mice and littermate control *Insr*^{wt/wt},*Ins1*^{cre/wt},nTnG mice were generated using a breeding scheme to ensure consistency of the Cre donor parent (Fig. 1C). Cre-recombinase efficiency was assessed using the nuclear TdTomato-to-nuclear EGFP (nTnG) lineage trace reporter (Prigge et al., 2013) and found to be robust on the *Insr*^{f/f},*Ins1*^{cre/wt},nTnG genetic background (Fig 1D). We confirmed by Western blotting that *Insr* protein was almost completely absent from β /*Insr*^{KO} islets and partially reduced from β /*Insr*^{HET} (Fig. 1E). qPCR showed that *Insr* mRNA was not decreased in any of the 18 tissues examined, including the whole brain or hypothalamus specifically, hence we did not perform Western blots for other tissues

(Fig. 1F). Together with other published data on *Ins1^{cre}* mice, these data strongly suggest that *Insr* deletion with *Ins1^{cre}* is robust and sufficiently specific to pancreatic β-cells.

Loss of β-cell Insr alters gene expression in purified β-cells

To establish a baseline gene expression profile of our β-cell specific *Insr* knockout model we performed an unbiased global analysis of β-cell gene expression in FACS purified GFP-positive β-cells labelled with the nTnG reporter (Fig. S1A). RNA sequencing revealed significant differences in mRNA expression between $\beta/\text{Insr}^{\text{KO}}$ β-cells and wild type β-cells (Fig. 2; Fig. S1B-E). Overall, differentially expressed genes were enriched in Reactome pathways related to NFκB signaling, Ras signaling, and mRNA splicing (Fig. S1B). In many cases, *Insr* gene deletion showed a gene-dose-dependent effect on regulated gene expression meaning that heterozygous $\beta/\text{Insr}^{\text{HET}}$ β-cells exhibited intermediate expression of target genes between the full *Insr* knockout and wildtype β-cells (Fig. S1C).

Significantly upregulated individual mRNAs in $\beta/\text{Insr}^{\text{KO}}$ mice included genes that promote insulin secretion (*Jak2*, *Atp6ap2*), mediate cell death (*Tmem123*, *Dusp26*, *Rela*) and mitochondria fragmentation (*Cers6*), and repress β-cell maturity (*Dusp26*) and proliferation (*Rela*, *Kras*), or participate in islet development (*Tm4sf4*) (Anderson et al., 2011; Chamberlain et al., 2014; Dai et al., 2015; Gomez-Banoy et al., 2019; Ma et al., 2001; Mandrup-Poulsen, 2003; Zhang et al., 2006). Several of the upregulated individual genes have been reported to be significantly associated with glycemic or obesity traits in human GWAS studies, including *Utp3*, *Rela*, *Cers6*, *Rnf6*, and *Tbce* (Fig. S1C; www.type2diabetesgenetics.org). Collectively, these upregulated genes point to β-cells that may be hyper-secretory, but are perhaps more susceptible to some stress conditions.

Individual genes that were significantly decreased included regulators of β-cell function, including the regulation of K_{ATP} channels, and β-cell fate (*Brsk2*, *Rab3a*, *Bmpr2*, *Camk2b*, *Mapk8ip3*), a negative regulator of Glut2 protein abundance (*Prnp*), a regulator of endocytosis (*Vps8*), a mediator of autophagy and cellular cholesterol traffic (*Gramd1a*), an anti-apoptosis gene (*Rel*), a transducer of ER stress (*Atf6b*), and a histone methyltransferase and STAT target gene (*Mettl8*) (Ashok and Singh, 2018; Engin et al., 2013; Fornoni et al., 2008; Frau et al., 2017; Goulley et al., 2007; Gu et al., 2018; Kline et al., 2013; Laraia et al., 2019; Locke et al., 2015; Mokhtari et al., 2009; Tobi et al., 2018; Wang et al., 2005; Yaekura et al., 2003; Yang et al., 2015; Zhang et al., 2001). Several of these downregulated genes showed strong evidence for genome-wide association with glycemic traits, including *Ttl12*, *C2*, *Atf6b*, *Sympk*, and *Camk2b* (Fig. S1C). Interestingly, *Ddx31* is a genetic regulator of circulating proinsulin levels in women but not men (Strawbridge et al., 2011). *Hnf4g* belongs to a network of transcription factors that play essential roles in β-cell function and fate but its specific role is unclear (Hara et al., 2000). Together, analysis of upregulated and downregulated genes points to the possibility that β-cells lacking *Insr* may exhibit increased glucose-stimulated insulin secretion but increased susceptibility to stress.

We also used unbiased protein-protein interaction network analysis to examine the relationships between the differentially expressed genes, as well as known components of the insulin signaling pathways. We identified key network hubs downstream of β-cell *Insr* (Fig. S1D). We also predicted the transcriptional regulators of *Insr*-regulated differentially expressed genes. Of these transcription factors *Rel*, *Pygo2*, *Polr2a*, *Nanos1* were significantly decreased and *Jak2*, *Thap3* significantly increased in *Insr*-deficient β-cells. These are likely to be the more proximal mediators of the *Insr*-dependent transcriptional program in β-cells (Fig. S1E).

Loss of β-cell Insr increases β-cell excitability

The RNA-seq analysis of *Insr*-regulated genes implicated multiple factors known to promote insulin secretion, including regulators of Glut2, mitochondria, K_{ATP} channels, and granule trafficking. We did not observe significant differences in the intensity or gross localization of Glut2 protein using immunofluorescence imaging (Fig. 3A,B). We examined mitochondrial function using the Seahorse bioanalyzer and found no significant differences between groups in females. In males, we observed a significant reduced oxygen consumption rate in dispersed islets from both $\beta/\text{Insr}^{\text{KO}}$ and $\beta/\text{Insr}^{\text{HET}}$ in comparison to controls during basal respiration and after antimycin A/rotenone injections, suggesting reduced ATP production (Fig. 3C). Insulin administration has been reported to open β-cell K_{ATP} channels, mediating negative feedback on insulin secretion (Khan et al., 2001). Lack of this endogenous insulin action through *Insr* would therefore be expected to lead to β-cell hyper-excitability in our mouse model in the context of high glucose. Indeed, electrophysiological analysis of single β-

cells from female $\beta/\text{Insr}^{\text{KO}}$ mice confirmed a significant increase in action potential firing frequency during glucose stimulation, when compared to control β -cells, with no differences in resting potential, firing threshold, or action potential height (Fig. 3D,E). The reversal potential was right-shifted in $\beta/\text{Insr}^{\text{KO}}$ β -cells, further suggesting reduced K^+ conductance (Fig. 3G). Interestingly, the hyper-excitability was observed in *Insr* knockout β -cells from female, but not male mice (Fig. 3E,F). Perhaps the reduced mitochondrial efficiency in males prevented β -cell hyperexcitability. It is also possible that male control β -cells were already maximally insulin resistant when studied. No significant differences have been identified in *Insr* mRNA expression between sorted β -cells from female and male islets (Stancill et al., 2019). We did not observe a statistically significant difference in depolarization induced exocytosis in single cells from either sex (Fig. 3H), suggesting that the late stages of insulin granule exocytosis are not altered under these conditions.

Next, we analyzed Ca^{2+} responses to 15mM glucose in thousands of Fura-2-loaded dispersed islet cells and analyzed the data with an adaptation of our TraceCluster algorithm (Wills et al., 2016). In agreement with the electrophysiological data, *Insr* knockout β -cells from female mice exhibited a significantly greater number of oscillation peaks within the glucose stimulation period compared to control cells (Fig. 3I,J, S2). A similar increase in excitability was observed in $\beta/\text{Insr}^{\text{HET}}$ β -cells. Collectively, these experiments demonstrate that β -cells lacking *Insr* have increased electrical activity, suggesting that insulin has a negative feedback influence on excitability in the context of hyperglycemia.

*Loss of β -cell *Insr* causes insulin hypersecretion in the context of stimulatory glucose*

Insulin secretion is driven by electrical excitability, so we next carefully examined the effects of partial and full β -cell *Insr* deletion on secretory function employing multiple orthogonal *in vitro* and *in vivo* assays. We used islet perfusion to examine the dynamics of insulin secretion *ex vivo* at rest (3 mM glucose) and in response to 20mM glucose or 10mM glucose, as well as direct depolarization with 30mM KCl. Islets from female 16 week-old $\beta/\text{Insr}^{\text{KO}}$ and $\beta/\text{Insr}^{\text{HET}}$ mice secreted more insulin in response to 20 mM glucose and 30 mM KCl compared to islets from control mice (Fig. 4A). No significant differences were observed at 3mM or 10mM glucose (Fig. 4A). Consistent with our electrophysiology data, we did not observe differences in islets from males of the same age and on the same diet (Fig. 4B). It seems possible that reduced ATP generation in male mice (Fig. 4C) offsets any enhanced excitability/ Ca^{2+} responsiveness, to result in absence of significant changes in insulin secretion.

This potentiation of high glucose-stimulated insulin secretion *ex vivo* in the complete and partial *Insr* knockout β -cells, led us to examine how insulin levels were affected by glucose stimulation *in vivo* using the hyperglycemic clamp technique in awake mice. For this cohort of mice, there were no significant differences in body mass (control 20.5 +/- 0.5g n=8 vs $\beta/\text{Insr}^{\text{KO}}$ 20.8 +/- 0.4g n=10), lean mass (control 17.5 +/- 0.4g vs $\beta/\text{Insr}^{\text{KO}}$ 17.3 +/- 0.2g), or fat mass (control 1.8 +/- 0.3g vs $\beta/\text{Insr}^{\text{KO}}$ 2.2 +/- 0.2g). Glucose infusion rates were adjusted in order to reach hyperglycemic levels (~19 mM) in $\beta/\text{Insr}^{\text{KO}}$ and wild type control mice (Fig. 4C, D, G, H). Interestingly, slightly higher glucose infusion rates were necessary in female $\beta/\text{Insr}^{\text{KO}}$ mice in comparison to control mice in order to reach similar hyperglycemic levels (Fig. 4C). In accordance with our *ex vivo* insulin secretion data, glucose-stimulated insulin secretion was higher in female, but not in male $\beta/\text{Insr}^{\text{KO}}$ mice compared with control mice (Fig. 4E, I). We further tested whether *in vivo* insulin secretion would be potentiated after a single bolus of glucose in mice with reduced β -cell *Insr*. At 11 weeks of age, plasma insulin response, relative to baseline, was significantly elevated 30 min after i.p. injection of 2g/kg body mass glucose in female, but not in male, $\beta/\text{Insr}^{\text{KO}}$ mice compared to controls (Fig. 4K, L). In accordance with the electrophysiology, Ca^{2+} oscillation, and islet perfusion data, we detected no statistical difference between female genotypes in fasting plasma insulin *in vivo* at multiple ages (Fig. S3). Together, these experiments suggest that β -cell *Insr* can play suppressive role in glucose-stimulated insulin secretion without much impact on basal insulin secretion.

*Effects of β -cell *Insr* loss on insulin production, storage, processing and clearance*

Insulin and insulin signaling can modulate protein synthesis in many cell types and we have previously provided evidence that soluble cellular insulin protein transiently increases in human islet cell cultures treated with exogenous insulin (Luciani and Johnson, 2005). To assess the quantitative contribution of *Insr* signaling to insulin production and mRNA translation rates we measured total islet

insulin content after acid-ethanol extraction and examined total protein synthesis rate using S^{35} -methioione/cysteine pulse labelling in isolated islets. Total insulin content and protein synthesis in isolated islets were unaffected by *Insr* deletion under these basal glucose conditions (Fig. 5M-P).

To investigate the role of *Insr* signaling on β -cell stress and insulin clearance, we conducted analysis of plasma proinsulin to C-peptide ratios, and C-peptide to insulin ratios in the fasting state (4h) across multiple ages in both male and female mice, and on multiple diets (Fig. S4). While many of these parameters changed with age, no statistical differences between genotypes was seen in any of these parameters of mice fed either a low-fat diet (LFD) or a high fat diet (HFD). A trend towards lower insulin clearance was observed in LFD-fed female $\beta/\text{Insr}^{\text{KO}}$ mice in comparison to wild type control mice at 7 weeks. Collectively, these experiments show that β -cell insulin receptor signaling has only a small, if any, effect on insulin processing and clearance at baseline glucose conditions.

Beta-cell area and hyperglycemia-induced proliferation in mice lacking β -cell *Insr*

As our RNA sequencing data revealed pathways downstream of *Insr* signaling that may affect β -cell proliferation capacity (Fig. 2), we examined baseline β -cell area and proliferation reserve capacity. Islet architecture and β -cell-to- α -cell ratio were not obviously perturbed (Fig. 5A). We did not detect significant differences associated with genotype in β -cell area in either female or male mice, at 13, 42 weeks (LFD) or 54 weeks (HFD) of age (Fig. 5B). In comparison to control mice, HFD fed female $\beta/\text{Insr}^{\text{KO}}$ mice had a tendency toward a smaller β -cell area at 54 weeks of age that were consistent with tendencies towards lower plasma insulin (Fig. S3C), proinsulin and C-peptide levels (Fig. S4). These data suggest that *Insr* may help support age-dependent β -cell expansion under some conditions.

Prolonged hyperglycemia can stimulate β -cell proliferation in adult mouse β -cells (Sharma et al., 2015), but whether this requires intact insulin receptor signaling remains controversial. To examine the role of *Insr*-mediated signaling on hyperglycemia-induced β -cell proliferation, we performed 4-day hyperglycemic infusions in $\beta/\text{Insr}^{\text{KO}}$ and wild type control mice. In female mice, hyperglycemia (>10 mM; Fig. 5F) resulted in mildly elevated insulin secretion in $\beta/\text{Insr}^{\text{KO}}$ relative to control mice for the initial 48 h, which was not sustained for the duration of the experiment (Fig. 5G,H), while glucagon levels declined similarly in both genotypes (Fig. 5I,J). There was no effect of *Insr* deletion on hyperglycemia-induced proliferation of either β -cells or α -cells in females (Fig. 5K,L). In male mice, 96 h of hyperglycemia resulted in sustained hyperinsulinemia in $\beta/\text{Insr}^{\text{KO}}$ mice (Fig. 5M-O), with no differences in circulating glucagon (Fig. 5P,Q). In male mice lacking β -cell *Insr*, this manipulation was associated with more β -cell proliferation (Fig. 5R,S). The fact that we did not observe a suppression of glucose-induced proliferation of β -cells lacking *Insr* prompted us to determine the degree to which the broadly defined insulin signaling pathway was inhibited in our model. Indeed, glucose-induced Akt phosphorylation, shown by western blot of whole islet lysate, was statistically unaffected, and glucose-induced Erk phosphorylation was only reduced ~50% in *Insr* knockout β -cells (Fig. 5T). It is likely that the *Igf1r* or a receptor tyrosine-kinase-independent mechanism initiates parts of intracellular post-receptor ‘insulin signaling’ in the absence of *Insr*. Testing this hypothesis in the future will require truly β -cell specific double deletion of *Insr* and *Igf1r*.

Modelling contributions of peripheral and β -cell specific insulin sensitivity to glucose homeostasis

The continuum between insulin sensitivity and resistance impacts multiple tissues, including pancreatic β -cells. We observed that β -cell-specific insulin resistance resulted in insulin hypersecretion in the context of unchanged β -cell mass. We next used mathematical modelling to generate quantitative predictions of the dependence of glucose tolerance on both β -cell and whole-body insulin resistance, both independently and synchronously. As described in the methods section, we modified the Topp model (Topp et al., 2000) to include insulin receptor-mediated negative feedback on insulin secretion, as indicated by our experimental data, with S_{β} serving as the β -cell *Insr*-specific insulin sensitivity parameter (see equations in Fig. 6A; for $\beta/\text{Insr}^{\text{KO}}$ mice, $S_{\beta} = 0$). Peripheral insulin sensitivity is represented by S_P , (S_I in the original Topp model). We used our hyperglycemic clamp data (Figs. 4C-H, S5A,B) to estimate S_{β} in both female and male control mice and found $S_{\beta,\text{female}}$ to be significantly different from zero ($S_{\beta,\text{female}} = 3.4 +/ - 1.5 \text{ nM}^{-1}$, $p = 10^{-25}$) and significantly different from $S_{\beta,\text{male}}$ ($p = 10^{-24}$). $S_{\beta,\text{male}}$ was not significantly different from zero ($S_{\beta,\text{male}} = -0.05 +/ - 1.0 \text{ nM}^{-1}$, $p = 0.7$). *In silico* glucose tolerance tests found that decreased β -cell insulin-sensitivity (S_{β}) (similar to $\beta/\text{Insr}^{\text{KO}}$ mice) corresponded with elevated peak and plateau insulin secretion (Fig. 6B). As expected,

this was predicted to drive more rapid clearance of blood glucose (Fig 6C). Analysis of areas under the curve for glucose and insulin resulting from *in silico* glucose tolerance tests while varying S_p and S_β indicated that β -cell insulin resistance should have a marked effect on insulin secretion and glucose tolerance, most dramatically in conditions of low peripheral insulin sensitivity. Next, we compared the predictions of this model with experimental results. We used the *in silico* AUC_{Glucose} values as a function of both S_p and S_β combined with averaged experimental AUGC values to estimate S_p as a function of age for the low-fat diet conditions (Fig. S5C,D). We found that male values of S_p for wildtype and mutant were indistinguishable from each other while females showed significant differences from each other and from the male values at all ages. As expected, HFD led to reduced peripheral insulin sensitivity (Fig. S5E). Collectively, these simulations show how β -cell insulin sensitivity and peripheral insulin sensitivity may combine to the regulation of glucose tolerance.

*Condition-dependent improved glucose tolerance with reduced β -cell *Insr* signaling*

To test our theoretical model experimentally, we examined glucose tolerance in female and male $\beta\text{Insr}^{\text{KO}}$, $\beta\text{Insr}^{\text{HET}}$, and control littermates at multiple ages between 4 and 52 weeks in the context of two diets. Significant improvements in glucose tolerance were observed in female mice with reduced *Insr* signaling at multiple ages, and in young males (Fig. 6F). Consistent with our mathematical modelling that suggested a diminished contribution of β -cell insulin resistance to glucose homeostasis in the context of greater whole-body insulin resistance, we did not observe significant effects of genotype in older male mice, or mice of either sex fed an insulin-resistance-inducing HFD (Fig. 6F). Thus, *Insr* deletion has little consequence on glucose tolerance in mice with already impaired pan-tissue insulin resistance, which we and others have shown increases with age and is more pronounced in male mice (Fig. S5).

The *Ins1*^{cre} allele results in pre-natal gene deletion (Thorens et al., 2015). To assess the effects of *Insr* deletion in adult β -cells, and to determine the role of *Insr* on a different genetic background and under different housing conditions, we also phenotyped multiple cohorts of mice in which the *Insr*^{fl/fl} allele was recombined by the *Ins1* promoter-driven CreERT transgenic allele (commonly known as MIP-Cre) after injection with tamoxifen. In agreement with our observations in mice with constitutive loss of β -cell *Insr*, we found that glucose tolerance was significantly improved 4 weeks after β -cell-specific *Insr* deletion in male mice (Fig. 6G). These differences were not maintained as the mice aged and presumably became more insulin resistant. In these mice, there were no significant differences observed in fasting glucose (control 4.8 +/- 0.3mM n=7 vs $\beta\text{Insr}^{\text{KO}}$ 4.4 +/- 0.2mM n=10), β -cell mass (control 1.4 +/- 0.3% n=3 vs $\beta\text{Insr}^{\text{KO}}$ 2.1 +/- 0.2% n=5), or body mass (control 26.1 +/- 1.1g n=7 vs $\beta\text{Insr}^{\text{KO}}$ 23.1 +/- 0.7g n=17). Collectively, these observations using an independent model and independent housing conditions lend support to our conclusion that the initial consequence of β -cell specific *Insr* deletion is improved glucose tolerance.

*Peripheral effects of β -cell specific *Insr* loss*

We and others have shown that even modest differences in hyperinsulinemia can have profound consequences for insulin sensitivity, adiposity, fatty liver, longevity and cancer (Mehran et al., 2012; Templeman et al., 2017; Zhang et al., 2019). Thus, we asked how the context-dependent glucose-stimulated insulin hyper-secretion induced by targeted β -cell specific insulin resistance may affect insulin sensitivity, adiposity, and body mass over time. Insulin sensitivity was assessed at multiple ages in the same mice. Interestingly, insulin sensitivity was significantly improved in 10-week-old female $\beta\text{Insr}^{\text{HET}}$ mice compared to littermate controls without *Insr* deletion (Fig. S6). On a high fat diet, male $\beta\text{Insr}^{\text{KO}}$ and $\beta\text{Insr}^{\text{HET}}$ mice had significantly improved insulin sensitivity compared to controls at 22 weeks of age. Longitudinal tracking of 4-h fasting glucose identified relative hypoglycemia in young LFD female $\beta\text{Insr}^{\text{KO}}$ and $\beta\text{Insr}^{\text{HET}}$ mice, older LDF male $\beta\text{Insr}^{\text{KO}}$ and $\beta\text{Insr}^{\text{HET}}$ mice, and across the tested ages in HFD female mice (Fig. 7A-D). Longitudinal tracking of body weight revealed that female mice with reduced β -cell *Insr* consistently weighed more than controls when fed a HFD (Fig. 7E-H), consistent with the known role of hyperinsulinemia in diet-induced obesity (Mehran et al., 2012; Templeman et al., 2015). We also examined the mass of several tissues at 13 weeks of age. Interestingly, liver mass was lower in both female and male mice lacking β -cell *Insr* (Fig. 7IJ). Pilot experiments showed that liver *Insr* protein abundance appeared reduced in mice with partially or completely reduced β -cell *Insr*, in the context of the LFD but not the HFD (Fig. 7K). These data are

consistent with the concept that modest hyperinsulinemia can drive down insulin receptor levels and the concept that insulin signaling is a trophic signal for liver. Together, these data demonstrate that specifically preventing autocrine insulin feedback can have systemic effects on insulin sensitivity, body mass, and the size of some tissues. These changes may affect the eventual susceptibility to type 2 diabetes.

Discussion

The goal of the present study was to establish the role of β -cell specific insulin resistance on β -cell function and glucose homeostasis using specific genetic loss-of-function tools. We found that *in vivo* *Insr* deletion potentiated glucose-stimulated insulin secretion by increasing action potential firing and Ca^{2+} oscillation frequency, leading to improved glucose tolerance in insulin sensitive animals. Our data therefore suggest a model in which insulin inhibits its own secretion in a context-dependent manner and that this local negative feedback loop has physiological consequences for glucose tolerance.

Autocrine signaling in endocrine cells is generally a negative feedback (Norman and Henry, 2014), with a few exceptions in specific conditions (Ma et al., 2005). Given the abundance of *Insr* protein in islets and the physiological modulation of both insulin and *Insr* signaling in health and disease, autocrine and paracrine insulin signaling have been topics of interest and controversy for decades (Braun et al., 2012; Leibiger et al., 2008). While some have questioned whether local insulin levels are sufficient for signaling within the islet, mathematical modelling of insulin hexamer dissolution estimated that monomeric insulin within islets is in the picomolar range (Wang et al., 2013), similar to the dose that maximally activates insulin signaling pathways (Alejandro et al., 2010; Beith et al., 2008). Consistent with a narrow range of responsiveness, our results also show that the contribution of autocrine insulin feedback to glucose homeostasis depends on whether mice are on a diet or at an age where insulin resistance is high, and potentially saturated in β -cells. Background genetics, diet, housing conditions, microbiome, or glucose concentrations could contribute to differences in observed phenotypes between our β -cell specific *Insr* knockout models and the frank diabetes reported for transgenic models that use fragments of the *Ins2* or *Pdx1* promoters to drive Cre-mediated β -cell *insr* deletion (Kulkarni et al., 1999; Okada et al., 2007; Otani et al., 2004). However, we believe that the discrepancy is more likely due to depletion of *Insr* in key neuronal populations since both of *Ins2* and *Pdx1* are expressed in brain regions that influence glucose homeostasis (Vogt and Bruning, 2013; Wicksteed et al., 2010a). For example, *Insr* deletion in the brain with Nestin Cre causes insulin resistance (Plum et al., 2005) and impairs the sympathoadrenal response to hypoglycemia (Fisher et al., 2005), while *Insr* knockout using AgRP Cre results in abnormal suppression of hepatic glucose production (Konner et al., 2007). We expect that our β -*Insr*^{KO} mouse line is the most tissue specific model used to date for the study of autocrine insulin signaling and β -cell insulin resistance.

Using genetic and genomic tools, our work complements previous studies in humans and animal models. *Ex vivo* studies of perfused canine pancreata found an inhibitory autocrine effect of insulin (Iversen and Miles, 1971). Similarly, exogenous insulin perfusion of canine pancreas *in situ* was shown to lead to reduced endogenous insulin production (Rappaport et al., 1972). *In vivo* insulin infusion rapidly suppressed C-peptide levels in healthy men, but not those with obesity and presumably global insulin resistance (Cavallo-Perin et al., 1993). In isolated human islets, perfusion studies showed that treatment with physiological doses of insulin had no effect on C-peptide release (Johnson and Misler, 2002b), while static incubation experiments found only moderate potentiation of glucose-stimulated insulin secretion with super-physiological levels of insulin (Braun et al., 2012). Our conclusions are in line with the recent work of Paschen et al reporting that a high fat, high sucrose diet induced tissue-selective insulin resistance in β -cells, as well as profound hyperinsulinemia and β -cell hyper-excitability (Paschen et al., 2019). Our mechanistic finding that *Insr* knockout β -cells have increased action potential firing frequency is consistent with previous observations that insulin directly increased K_{ATP} currents via PI3-kinase signaling (Khan et al., 2001) and that PI3-kinase inhibition with wortmannin potentiates glucose stimulated insulin secretion in normal, but not T2D, human islets (Kolic et al., 2016). Our studies further illustrate the molecular mechanisms of negative autocrine feedback in β -cells during high glucose stimulation.

Beyond the potentiation of glucose-stimulated insulin secretion, transcriptomic analysis of fully and partially *Insr*-deficient β -cells revealed a broad re-wiring of multiple signaling pathways and gene networks that are expected to change how these cells respond to stresses. In particular, *Insr* loss in

our model biased the combined insulin/Igf signaling pathway towards Ras/MAP-kinase signaling and increased in the capacity for cytokine signaling that could modulate cell fate. The conditions under which these gene expression changes could manifest in β -cell proliferation or increased β -cell survival remain incompletely explored. Otani et al reported modestly reduced β -cell mass in non-diabetic *Irs2-Cre* transgenic *Insr* knockouts, which was exacerbated by diabetes, but they did not employ Cre controls (Otani et al., 2004). Okada et al reported impaired compensatory β -cell proliferation in the context of high fat diet or liver *Insr* knockout in the same experimental groups (Okada et al., 2007). These previous studies comparing β -cell knockout mice of *Insr* versus *Igf1r*, suggested a more important role for the former in β -cell proliferation and survival (Okada et al., 2007). Insulin receptor over-expression experiments also support the idea that β -cells are key insulin targets (Okamoto et al., 2004). In the present study, we were unable to identify conditions which would result in statistically significant differences in β -cell mass in mice with *Insr* deficiency, but variability was high and relatively few animals were studied at older ages. We have previously shown that the increase in β -cell mass resulting from high fat diet requires local insulin production and is independent of hyperglycemia (Mehran et al., 2012), consistent with the known direct anti-apoptotic and mitogenic effects of insulin *in vitro* (Beith et al., 2008; Johnson et al., 2006a; Muller et al., 2006). These findings can be reconciled by proposing that high insulin concentrations within the islet are sufficient to activate remaining *Igf1* receptors linked to biased post-receptor signaling. We observed that sustained hyperglycemia and hyperinsulinemia over 4 days was associated with increased proliferation, but whether these are effects are mediated through *Igf1r* function compensation will require double receptor knockout experiments. It is also possible that hyperglycemia itself is a major driver of β -cell proliferation under these conditions, through *Irs2-Creb* signaling that may bypass *Insr/Igf1r* (Jhala et al., 2003). It has also been demonstrated that ~80% of the gene expression changes attributed to glucose in MIN6 cells require full insulin receptor expression (Ohsugi et al., 2005). We have previously found that glucose cannot stimulate primary mouse β -cell proliferation when autocrine insulin signaling is blocked by somatostatin and that 'glucose-induced' Erk phosphorylation requires full insulin secretion (Alejandro et al., 2010; Beith et al., 2008). On the other hand, inhibiting *Insr* in mouse islets with S961 or shRNA did not block glucose-induced proliferation of cultured β -cells (Stamateris et al., 2016). Additional future studies will be required to resolve this controversy.

Early hyperinsulinemia is a feature of β -cell *Insr* knockout models on multiple genetic backgrounds (Kulkarni et al., 1999; Okada et al., 2007; Otani et al., 2004), including the present study. Loss of *Irs1* or *Akt* function results in basal hyperinsulinemia and, in some cases, increased β -cell mass (Bernal-Mizrachi et al., 2004; Kido et al., 2000), mimicking the early stages in human diabetes. Our experiments begin to shed light on the systemic consequences of the hyperinsulinemia caused by β -cell-specific insulin resistance, which may be an early event in the pathogenesis of type 2 diabetes. Human data suggests that β -cell insulin resistance can be found in the obese state prior to hyperglycemia (Cavallo-Perin et al., 1993). We and others have shown that hyperinsulinemia contributes to insulin resistance and obesity (Mehran et al., 2012; Templeman et al., 2015), through multiple mechanisms including the down-regulation of insulin receptors (Knutson et al., 1983). We observed propensity for excessive diet-induced body mass gain in mice with β -cell specific insulin resistance, as well as *Insr* protein down-regulation in the liver. Thus, β -cell defects such as impaired autocrine feedback through *Insr* may contribute to insulin hypersecretion and accelerate the early stages of type 2 diabetes (Esser et al., 2020). In the later stages, the lack of pro-survival insulin signaling, perhaps in combination with other molecular defects, may contribute to failures in β -cell compensation and survival, thereby further accelerating the course of the disease (Gunton et al., 2005; Kulkarni et al., 1999; Ohsugi et al., 2005; Okada et al., 2007; Otani et al., 2003).

Our studies illustrate the power of using both females and males to study integrated physiology. Indeed, β -cell *Insr* loss led to increased β -cell action potentials, calcium oscillations, and glucose-stimulated insulin secretion in 16-week-old female mice, but not in age-matched males. No intrinsic sex differences of *Insr* mRNA levels were in a transcriptomic analysis of sorted β -cells (Stancill et al., 2019). Given the abundance of data showing more pronounced insulin resistance in males (Parks et al., 2015; Yki-Jarvinen, 1984), the most likely reason for these female-specific phenotypic responses to β -cell *Insr* deletion was the development of insulin resistance in control males but not in control females. To this point, glucose tolerance is improved in 4-week-old β /*Insr*^{KO} males, an age at which control males remain insulin-sensitive, and in male mice with acute loss of *Insr*. More work will be needed to confirm this possibility, and to determine factors in addition to sex hormones and sex

chromosomes that impact these sex differences in insulin sensitivity and glucose homeostasis (Mauvais-Jarvis, 2015). The sex-specific nature of phenotypes arising from our genetic manipulation of *Insr* in β-cells highlights the importance of including both sexes to accurately interpret data and to draw conclusions that will apply to both sexes.

While our study is comprehensive and employs the best genetic tools available today, this work has limitations. *Ins1^{Cre}* is the most β cell-specific Cre deletion strain available today (Thorens et al., 2015), but this fact does not preclude off-tissue effects that have yet to be discovered. Cre recombinase itself is not totally benign. These facts and our detailed comparison of *Ins1^{wt/wt}* mice with *Ins1^{Cre/wt}* mice (Figs. S7-10), highlight the importance of the Cre control group we employed throughout our studies. Recently, it was reported that some colonies of *Ins1^{cre}* mice exhibited some silencing via DNA hypermethylation at the *Ins1* locus and this was suggested as an explanation for discordance between the phenotypes compared to gene deletions using Pdx1-Cre and Ins2-Cre transgenic lines (Mosleh et al., 2020). In our study, we observed virtually complete recombination in β-cells and no evidence for off-tissue *Insr* deletion. We believe a major source of discrepancy with previously reported phenotypes stems from the propensity of previous promoter transgenic strains to recombine in the brain and robust expression of *Insr* throughout the brain. Another caveat of our experiments using β /*Ins1^{KO}* mice is that *Insr* is expected to be deleted from β-cells starting in late fetal development (Thorens et al., 2015). In our hands, tamoxifen-inducible *Ins1^{CreERT}* mice have insufficient β-cell specific recombination for *in vivo* physiological studies. Our validation experiments using the tamoxifen-inducible *Ins1-CreERT* address this limitation and confirm that β-cell insulin resistance improves glucose tolerance, at least under the initial insulin sensitive conditions. It should also be noted that, because we show that long-term deletion of *Insr* results in profound re-wiring of the β-cell transcriptome, the physiological changes can be the result of either direct or indirect action of *Insr* signaling. It should also be emphasized that, while we have deleted *Insr*, insulin can signal through Igf1r and Igf2r, especially at the higher concentrations predicted in the pancreas. A further caveat is that the molecular mechanisms involved in insulin secretion may be different in mouse and human β-cells (Rorsman and Ashcroft, 2018), although we note that direction of effect we surmise agrees with the majority of human and canine studies, indicating general agreement across species (Cavallo-Perin et al., 1993; Elahi et al., 1982; Iversen and Miles, 1971; Rappaport et al., 1972).

In conclusion, our work demonstrates a key modulatory role for autocrine insulin negative feedback and the lack thereof (i.e. β-cell resistance) in insulin secretion, glucose homeostasis and body mass, which depend on the physiological context studied. We hope our studies resolved longstanding and controversial questions about the local effect of insulin on β-cells, and lead to experimental and theoretical studies that incorporate *Insr*-mediated signaling in other islet cell types.

Materials and Methods

Bioinformatics

Human tissue-level proteome and transcriptome were downloaded from the ProteomicsDB resource (<https://www.proteomicsdb.org>) (Schmidt et al., 2018) in 2019 and sorted by relative protein abundance in Microsoft Excel. Publicly available human islet scRNASeq data were acquired from the panc8.SeuratData package and the SCTransform pipeline was followed to integrate the studies (Hafemeister and Satija, 2019). Expression data were normalized using the Seurat::NormalizeData function with default parameters and visualized using the Seurat::RidgePlot and Seurat::UMAPPlot functions, all from the Seurat package in R (Stuart et al., 2019).

Mouse model and husbandry

All animal protocols were approved by the University of British Columbia Animal Care Committee (Protocol A16-0022), the Institutional Animal Care and Use Committee of the University of Massachusetts Medical School (A-1991-17) and the University of Michigan Institutional Animal Care and use Committee, in accordance with national and international guidelines. Mice were housed at room temperature on a 12/12 light dark cycle at the UBC Modified Barrier Facility, unless otherwise indicated.

Ins1^{cre} mice were gifted to us by Jorge Ferrer (Thorens et al., 2015) (now commercially available, Jax #026801). The *Insr^{fl/fl}* allele (#006955) and the nuclear TdTomato-to-nuclear EGFP (nTnG) lineage tracing allele (Prigge et al., 2013) were obtained from Jax (#023035) (Bar Harbor, ME). We generated

two parental strains to avoid Cre effects during pregnancy; *Ins1*^{cre/wt}; *Ins1*^{f/wt} male mice and *Ins1*^{cre/wt}, nTnG^{+/+} female mice. These two parental strains were crossed in order to generate full littermate insulin receptor knockout *Ins1*^{f/f}; *Ins1*^{cre/wt}, nTnG^{-/-} (β / β *Ins1*^{KO}) mice, partial insulin receptor knockout *Ins1*^{f/wt}; *Ins1*^{cre/wt}, nTnG^{-/-} mice (β / β *Ins1*^{HET}), and their control groups *Ins1*^{wt/wt}; *Ins1*^{cre/wt}, nTnG^{-/-} mice (3 alleles of insulin) and *Ins1*^{f/f}; *Ins1*^{wt/wt}, nTnG^{-/-} mice (4 alleles of insulin). *Ins1*^f, *Ins1*^{cre}, and nTnG genotyping were done in accordance with Jax's recommendations using a ProFlex PCR system (Thermo Fisher Scientific, Canada). NNT genotyping was done as described previously (Nicholson et al., 2010). Master mix for genotyping included 0.5 μ M primers (Integrated DNA technologies), 2mM dNTPs (New England Biolabs, #N0447S), 0.5U DreamTaq DNA polymerase (Fisher Scientific, #FEREP0702). Agarose gels varied from 1-2.5% (FroggaBio, #A87-500G).

In our studies, mice were fed 1 of 3 diets: either a chow diet (PicoLab Mouse Diet 20-5058); a low-fat diet (LFD; Research Diets D12450B) containing 20% of kcal protein, 10% of kcal fat, and 70% of kcal carbohydrate including 35% sucrose, or; a high-fat diet (HFD; Research Diets D12492) containing 20% of kcal protein, 60% of kcal fat, and 20% of kcal carbohydrate including 10% sucrose.

MIP^{cre} mice were generously obtained from Dr Dempsey (Wicksteed et al., 2010b). The CAG-YFP reporter transgenic animals were from Jax (#011107). All animals were males that were intraperitoneally injected at 8 weeks of age for 5 consecutive days with tamoxifen (Sigma, T5648) freshly dissolved in corn oil (Sigma, C8267) with 3 injections at 200 mg/kg over a 1-week period.

Comparison of control genotypes

Before conducting our main study, we did a pilot experiment to determine whether the *Ins1*^{cre} knock-in mice had any phenotype on their own under both low fat and high fat diets, and we tracked both 'control' genotypes for the majority of our studies. Although *Ins1*^{wt/wt}; *Ins1*^{cre/wt}, nTnG and *Ins1*^{f/f}; *Ins1*^{wt/wt}, nTnG control mice exhibited generally similar phenotypes, we observed key differences that reinforced the rationale for using controls containing Cre and lacking 1 allele of *Ins1*, matching the experimental genotypes. For example, male HFD-fed *Ins1*^{f/f}; *Ins1*^{wt/wt}, nTnG mice showed significantly higher levels of plasma proinsulin in comparison to *Ins1*^{wt/wt}; *Ins1*^{cre/wt}, nTnG mice at 16 and 28 weeks of age (Fig. S7). At several ages, both LFD and HFD fed female *Ins1*^{f/f}; *Ins1*^{wt/wt}, nTnG^{-/-} mice exhibited trends toward slightly improved glucose tolerance (Fig. S8), most likely due to one extra allele of insulin, in comparison to *Ins1*^{wt/wt}; *Ins1*^{cre/wt}, nTnG mice. Insulin sensitivity was generally similar, although not identical (Fig. S9). Longitudinal tracking of body weight revealed a consistent tendency for mice with a full complement of insulin gene alleles to be heavier than mice in which 1 allele of *Ins1* had been replaced with Cre. With the statistical power we had available, female HFD-fed *Ins1*^{f/f}; *Ins1*^{wt/wt}, nTnG mice had significantly increased body mass at 11 and 16 weeks of age in comparison to *Ins1*^{wt/wt}; *Ins1*^{cre/wt}, nTnG mice (Fig. S10). Once we had established the effects of the *Ins1*^{cre} allele on its own, we used a breeding strategy ensuring that all pups were born with 3 insulin alleles to control for any effects of reduced insulin gene dosage (See Fig. 1C). This strategy gave us cohorts of: *Ins1*^{wt/wt}; *Ins1*^{cre/wt}, nTnG^{-/-} (β / β *Ins1*^{KO}) control mice, *Ins1*^{f/wt}; *Ins1*^{cre/wt}, nTnG^{-/-} (β / β *Ins1*^{KO}) β -cell specific *Ins1*^f heterozygous knockout mice, and *Ins1*^{f/f}; *Ins1*^{cre/wt}, nTnG^{-/-} (β / β *Ins1*^{KO}) β -cell specific *Ins1*^f complete knockout mice. In some studies, the nTnG allele was not present (see Figure legends).

Islet isolation and dispersion

Mouse islet isolations were conducted by ductal inflation and incubation with collagenase, followed by filtration and hand-picking as in our previous studies and following a protocol adapted from Salvalaggio et al. (Beith et al., 2008; Johnson et al., 2006a; Luciani and Johnson, 2005; Salvalaggio et al., 2002). 24h post islets isolations, islets were washed (x4) (Ca/Mg-Free Minimal Essential Medium for suspension cultures, Cellgro #15-015-CV), followed by gentle trypsinization (0.01%), and resuspended in RPMI 1640 (Thermo Fisher Scientific #11875-093), 10%FBS, 1%PS). Seeding were done either on glass cover slips or in 96-well plates according to the experimental procedure (see below).

Immunoblotting

50 islets per sample were washed in PBS twice and then lysed and sonicated in RIPA buffer (10mM HEPES, 50mM β -glycerol phosphate, 1% Triton X-100) supplemented with complete mini protease inhibitor cocktail (Roche, Laval, QC) and phosphatase inhibitors (2mM EGTA, 70mM NaCl, 347 1mM Na3VO4, and 1mM NaF). Protein concentration was measured using Micro BCA Protein

Assay Kit (ThermoFischer Scientific). 10 µg of total protein for each sample was separated by SDS-PAGE and transferred to Immun-Blot PVDF membrane (Bio-Rad Laboratories). Subsequently, membranes were blocked in I-Block (ThermoFischer Scientific) and probed with primary antibodies targeting *insr*-β subunit (1:1000, CST #3020S), ERK1/2 (1:1000, CST #4695), p-ERK1/2 (Thr202/Tyr204) (1:1000, CST #4370), AKT (1:1000, CST #9272), p-AKT (Thr308) (1:1000, CST #9275), ACTB (Novus Biologicals, NB600-501). Protein detection was performed by the use of the HRP-conjugated secondary antibodies: anti-rabbit (CST #7074) or anti-mouse (CST #7076) and Immobilon Forte Western HRP substrate (Millipore Sigma). Protein band intensity on exposed film was measured with Adobe Photoshop software.

Targeted gene expression analysis

Tissue samples were kept frozen during grinding using mortars and pestles. cDNA was synthesized using qScript™ cDNA synthesis kits (QuantaBio, #95047-500) following RNA was isolated from 50-100mg of sample using RNeasy mini kits (Qiagen, #74106) according to manufacturer's recommendations. qPCR was performed in 15ul reaction volumes using a CFX384 Touch Real-Time PCR Detection System (BioRad). Primer sequences: *Insr* forward 5'- 376 TTTGTCATGGATGGAGGCTA-3' and *Insr* reverse 5'-CCTCATCTGGGGTTGAAC-3'. *Hprt* forward 5'-TCAGTCAACGGGGACATAAA-3' and *hprt* reverse 5'-GGGGCTGT 379 ACTGCTTAACCAG-3'. *Insr* expression data were analyzed using the $2^{-\Delta\Delta CT}$ method using *Hprt* as a housekeeping gene. $\Delta Cq=Cq(Insr)-Cq(Hprt)$ followed by normalization of the $\Delta Cq(\text{exp})$ to the mean of the *Hprt* expression in liver.

RNA sequencing

To generate transcriptomic data from β-cells lacking *Insr* and littermate controls, groups of 50 islets were dispersed using mild trypsin digest according to our standard protocol (Alejandro et al., 2010; Luciani and Johnson, 2005), and FACS purified based on the GFP-positivity of the *Ins1*^{Cre}-induced nTnG allele. RNA isolation and library preparation were conducted in accordance with the SMART seq 2 protocol (Picelli et al., 2014). Sequencing of 100 GFP-positive β-cells was performed at the UBC Sequencing and Bioinformatics Consortium using Illumina NextSeq 500 with paired-end 75 bp reads. The number of read pairs per sample ranged from 4 millions to 42 millions with a median of 18 millions. Multiple analysis pipelines have been applied and their results combined using the procedure described elsewhere (Wang et al., 2019). One sample with exceptionally high glucagon reads was omitted, as a presumed β-cell purification failure. Pathway enrichment analyses were generated using Reactome and protein-protein interaction networks and subnetworks were derived using NetworkAnalyst 3.0 (<http://www.networkanalyst.ca/>) (Zhou et al., 2019).

Protein-protein interaction network, sub-network and TF-gene network was generated from differentially expressed genes between KO and WT control group using Network Analyst 3.0 platform (<http://www.networkanalyst.ca/>) (Zhou et al., 2019). PPI network data were based on STRING interactome with high (900-1000) confidence score. PPI sub-network enriching KEGG 'Insulin signaling pathway' was generated using the Module Extraction function. TF-gene network data were based on ENCODE ChIP-seq data.

Islet metabolism and oxygen consumption analysis

The Seahorse XF Cell Mito Stress Test kit (cat#103015-100) was used to measure oxygen consumption rate (OCR) in dispersed mouse islets using an Agilent Seahorse XF96 Analyzer XF96 (Seahorse Bioscience, North Billerica, MA). Dispersed islet cells were seeded at a density of 40,000 cells/well. 48h post seeding, additionally, 180µL of Seahorse XF Calibrant Solution (cat#100840-000) was added to each well of the Seahorse XF Sensor Cartridge to hydrate the XF Utility Plate (cat#102416-100). The hydrated cartridge was kept in a non-CO₂ incubator at 37°C for 24h hereby removing the CO₂ from media. To allow the assay media to pre-equilibrate, 180 µL of assay (eagle's minimal essential medium (DMEM, no glucose, Gibco, (cat#103334-100) supplemented with 25 × 10⁻³M glucose and 25 × 10⁻³M 4-(2-hydroxyethyl) -1-piperazinemethanesulfonic acid(HEPES)) was added to each well 1 h prior to the run and used for extracellular flux measurements ofXF. The plate was kept at 37 °C in a non-CO₂ incubator. Mitochondrial respiration was analyzed by sequential injections of modulators including oligomycin (1M) used to block ATP synthase, carbonyl-cyanide-4-(trifluoromethoxy) phenylhydrazone (FCCP 2.5M) to activate uncoupling of inner mitochondrial

membrane allowing maximum electron flux through the electron transport chain, and a mix of rotenone (1M) and antimycin A (1M) were used together to inhibit complexes I and III, respectively. The modulators were diluted in XF Assay Medium and loaded into the injection ports of the hydrated sensor cartridge corresponding to the order of injection 1 h prior to the run.

Patch-clamp electrophysiology

Islets from 16-week-old chow-fed male and female mice were isolated at UBC. 100-300 islets from each mouse shipped in a blinded manner overnight to the University of Alberta in RPMI (Invitrogen, 11875) with 10% FBS (Invitrogen #12483020), and 1% penicillin-streptomycin (Thermo Fisher, #15070063). Islets were dissociated into single cells using StemPro accutase (Thermo Fisher Scientific, Cat# A11105-01) one day after receiving the islets. Dispersed cells were cultured in RPMI-1640 containing 11.1 mM glucose with 10% FBS and 100 U/ml penicillin/streptomycin for up to 2 days.

Membrane potential and current measurements were collected using a HEKA EPC10 amplifier and PatchMaster Software (HEKA Instruments Inc, Lambrecht/Pfalz, Germany) in either the current- or voltage-clamp mode in the perforated patch-clamp configuration. All the measures were done in a heated chamber (32–35°C). Membrane potential measurement was performed with patch pipettes pulled from thick-walled borosilicate glass tubes (Sutter Instrument), with resistances of 8–10 MΩ when filled with 76 mM K₂SO₄, 10 mM KCl, 10 mM NaCl, 1 mM MgCl₂ and 5 mM Hepes (pH 7.25 with KOH), and back-filled with 0.24 mg/ml amphotericin B (Sigma, cat# a9528). The extracellular solution consisted of 140 mM NaCl, 3.6 mM KCl, 1.5 mM CaCl₂, 0.5 mM MgSO₄, 10 mM Hepes, 0.5 mM NaH₂PO₄, 5 mM NaHCO₃, 5 mM glucose (pH 7.3 with NaOH). Membrane potential was measured with 5 mM G starting from the beginning, for 5 min, then changed to 1 mM G for 4-5 min, then changed to 10 mM G for 8-10 min, finally changed back to 5 mM G. K_{ATP} currents and reversal potential were recorded during and after membrane potential measurement on each cell. β-cells were distinguished by characteristic differences in the voltage-dependent inactivation of Na⁺ channel currents (Gopel et al., 2000).

Measurement of voltage-dependent exocytosis was performed in the whole-cell configuration. Before the start of whole-cell patch clamping, media were changed to bath solution containing (in mM): 118 NaCl, 20 Tetraethylammonium-Cl, 5.6 KCl, 1.2 MgCl₂, 2.6 CaCl₂, 5 HEPES, and 5 glucose (pH 7.4 with NaOH). For whole-cell patch-clamping, fire polished thin-walled borosilicate pipettes coated with Sylgard (3-5 MΩ), contained an intracellular solution with (in mM): 125 Cs-glutamate, 10 CsCl, 10 NaCl, 1 MgCl₂, 0.05 EGTA, 5 HEPES, 0.1 cAMP, and 3 MgATP (pH 7.15 with CsOH). Quality control was assessed by the stability of seal (>10 GΩ) and access resistance (<15 MΩ) over the course of the experiment. Data were analysed using FitMaster (HEKA Instruments Inc) and Prism 6.0h (GraphPad Software Inc., San Diego, CA).

Calcium imaging and analysis

Two days following cell seeding on glass coverslips, adherent islet cells were loaded with 5 μM of the acetoxyethyl (AM) ester form of the calcium indicator Fura-2 (Thermo Fisher Scientific #F1221) for 30min. Islet cells were perfused at 1mL/min for 45min prior to experimental procedure to ensure washout of excess FURA2. During experiments, cells were mounted on a temperature-controlled stage and held at 37°C on a Zeiss Axiovert 200M inverted microscope equipped with a FLUAR 20× objective (Carl Zeiss, Thornwood, NY), while perfused with Krebs-Ringer (KRB) solution (144mM NaCl, 5.5mM KCl, 1mM MgCl₂, 2mM CaCl₂, 20mM HEPES) of various glucose concentrations as indicated in figures.

Ca²⁺ traces were analyzed automatically, as follows. Taking a similar approach to that described previously (Wills et al., 2016), 8 features were extracted from the Traces (Fig S2). Peaks during each phase were identified as local maxima reaching a value with a percent difference above the median baseline level greater than 20%. P-values for calcium analysis were generated using ANOVA with correction for multiple comparisons performed using Tukey's method. Figures were generated using the ggplot2 package in R (Wickham2016). Code used to analyze data and generate figures are available upon request.

Analysis of total protein synthesis rate

For the purpose of pulse labeling of newly translated proteins, 50 isolated islets were incubated in complete RPMI media without cysteine and methionine (MP Biomedicals, #SKU 091646454) for 1hr.

Subsequently media was supplemented with 250 μ Ci of [35 S]-cysteine/methionine mixture (PerkinElmer, NEG772002MC) and islets were incubated under normal conditions for 30 min. Islets were then lysed and proteins separated by SDS-gel electrophoresis as described above. Gels were fixed for 30 min in 50% (v/v) ethanol in water with 10% (v/v) acetic acid, dried in gel dryer (Bio-Rad model 583) and then exposed to storage phosphor screen (GE Healthcare) overnight. Screens were imaged and digitised using Typhoon FLA 9000 biomolecular imager (GE Healthcare). Protein bands intensity was quantified with Adobe Photoshop software.

Dynamic insulin secretion perifusion analysis

For perfusion experiments, islets from 16 week old chow-fed male and female mice were isolated using collagenase, filtration and hand-picking as previously described (Johnson et al., 2006b). Our standard approach compared the insulin response to both 20 mM and 10 mM glucose stimulation as well as direct depolarization with 30 mM KCl. More specifically, 150 hand-picked islets per column were perfused (0.4 mL/min) with 3 mM glucose KRB solution containing (in mM) 129 NaCl, 4.8KCl, 1.2 MgSO₄•7H₂O, 1.2 KH₂PO₄, 2.5 CaCl₂, NaHCO₃, 10 HEPES, as well as 0.5% BSA (Sigma # A7030) for 60 min to equilibrate the islets to the KRB and flow rate, and then treated as indicated. Samples were analyzed using a rat insulin radioimmunoassay that has 100% cross-reactivity for mouse insulin (Millipore-Sigma #ri-13k). Insulin content was measured after acid-ethanol extraction using an insulin ELISA (Stellux Rodent Insulin ELISA, Alpco #80-INSMR-CH10).

Hyperglycemic clamps

In vivo hyperglycemic clamp experiments were performed at the National Mouse Metabolic Phenotyping Center (NMMPC) at UMass Medical School. Body composition analysis was conducted by noninvasively measuring whole body fat mass and lean mass using ¹H-MRS (Echo Medical Systems, Houston, TX). A survival surgery was performed at 5–6 days before hyperglycemic clamp experiments to establish an indwelling catheter in the jugular vein. On the day of experiment, mice were fasted overnight (~15h), and a 2-h hyperglycemic clamp was conducted in awake mice by intravenously infusing 20% dextrose to rapidly raise and maintain plasma glucose levels at ~19 mM (Zhang et al., 2012).

Intravenous 4-day glucose infusion

Mice were bred and genotyped at University of British Columbia and shipped at 5 weeks of age to the Division of Diabetes, Department of Medicine, University of Massachusetts Medical School, USA. In a blinded manner, glucose infusions were performed as described (Alonso et al., 2007). Jugular vein catheters were placed in 9–12-week-old male and female mice with blinded genotypes. From postoperative recovery through euthanasia mice were unrestrained and were maintained on a 12-h light/dark cycle, with access to 2.2 g diet (to ensure isocaloric intake across all mice) and water. After 2 days of recovery, mice received continuous 4-day intravenous infusions of 50% dextrose (Baxter) containing 500 ug/mL BrdU. Tail blood was sampled for plasma insulin, glucagon and blood glucose at Day 0, 1, 2 and 4. Blood glucose was measured using ReliOn glucometer (Walmart), glucagon was measured using mouse Glucagon ELISA (Mercodia 10-1281-01), and plasma insulin was measured using mouse Insulin ELISA kit (Mercodia 10-1247-01). Mice were euthanized at the end of the experiment and pancreas and duodenum were harvested for histology. Tissues were fixed for 5 h in 10% formalin and then stored in 1X PBS until processing, paraffin embedding and sectioning. Images were acquired using a NIKON fully motorized for Phase and Fluorescence Ti-E microscope. Images were taken of at least 10 randomly selected islets, all four channels at the same time. To generate RGB images, channels were inserted to show Insulin-BrdU-DAPI, Glucagon-BrdU-DAPI or Insulin-Glucagon-DAPI. To generate yellow-magenta-white images to accommodate colorblind viewers, new files were generated in Adobe Photoshop in which original channel data were displayed in multiple channels using the merge function (e.g. to change green to yellow, green channel data were added to both green and red channels; for more detailed information please contact LCA). Cells were counted using Cell profiler automated counting software from Broad Institute (Cambridge, MA); all counts were manually checked.

β -Cell Mass and immunohistochemistry

Pancreata were perfused, then fixed for 24h with 4% paraformaldehyde, and then washed twice with 70% ethanol prior to paraffin embedding and sectioning (5 μm) to obtain 5 different regions of the pancreas (100 μm apart) by WAXit Inc. (Vancouver, Canada). Paraffin was removed by 5 min xylene incubation steps. Sections were rehydrated in decreasing concentrations of ethanol and rinsed with water and PBS. Epitope retrieval was done either by immersing samples 10 mM citrate buffer, pH 6.0 for 15min at 95°C, or by transferring sections to prewarmed 1N HCl for 25 min at 37°C. Samples were washed with PBS twice and were either blocked for 10 min at room temperature (Dako protein block #X0909), or with goat block (GB) with Triton X-100 (10% BSA + 5% Goat Serum with 0.5% Triton X-100) for 1-4 h at room temperature. Samples were incubated overnight at 4°C in primary antibodies targeting anti-insulin (1:200 Abcam #Ab7872), anti-glucagon (1:100 Cell Signaling Technologies, #2760S), anti-BrdU (1:250, Abcam ab6326), anti-GLUT2 (1:1000, Milipore, #07-1402). Following 3 PBS washes (5 min each), samples were incubated for 30min or 1h at room temperature in secondary antibodies in a light-deprived humid chamber. Secondary antibodies applied were anti-rabbit Alexa Fluor-488 (1:200, Invitrogen, # A-11008), anti-rabbit Alexa-488 (1:200, Invitrogen, #A11034), anti-rat Alexa-594 (1:200, Invitrogen, #A11007), anti-guinea pig Alexa-647 (1:200, Invitrogen, #A21450), anti-guinea pig Alexa-594 (1:200, Invitrogen #A-11076). Samples were mounted with either VECTASHIELD Hard Set Mounting Medium (Vector labs, # H-1500) or Fluoroshield both containing DAPI (Sigma-Aldrich, #F6182-20ML) following an additional three washes in PBS (10 min each). For β -cell area quantification, whole pancreas sections were imaged using an ImageXpress^{MICRO} using a 10x (NA 0.3) objective and analyzed using the MetaXpress software (Molecular Devices, San Jose, CA, USA). Beta cell area was calculated as insulin positive area normalized to the entire pancreas of each section. The mean of five sections from 5 regions of the pancreas were quantified. For other immunofluorescence analysis of fixed tissue, we used a Zeiss 200M microscope using 20x air objective (NA 0.75), NIKON fully motorized for Phase and Fluorescence Ti-E microscope. For live cell imaging for recombination validation, islets from *Ins1*^{cre/wt}:nTnG mice were incubated with CellMask™ Deep Red Plasma membrane stain (Invitrogen/Thermo Fisher - Catalog number: C10046) using a Leica confocal microscope.

Blood collection and *in vivo* analysis of glucose homeostasis and insulin secretion

Tail blood was collected for blood glucose measurements using a glucometer (OneTouch Ultra 2 meter, Lifescan, Canada) for single time points as well as during glucose and insulin tolerance tests. Mice were fasted for 4h or 16h during single timepoints and for 6h during glucose and insulin tolerance tests, as well as glucose stimulated insulin secretion tests. The *i.p.* glucose dose was 2g/kg unless otherwise specified. The *i.p.* Humalog (Eli Lilly and Co) insulin dose was 0.75U unless otherwise indicated. 1-2 days prior to femoral blood collection the experimental mice were tube handled and shaved. Femoral blood was collected for single timepoints, as well as for measurements of *in vivo* glucose-stimulated insulin secretion after *i.p.* injection of 2g/kg glucose. Blood samples were kept on ice during collection, centrifuged at 2000rpm for 10min at 4°C and stored as plasma at -20°C. Plasma samples were analysed for insulin (Stellux Chemi Rodent Insulin ELISA, Alpco #80-INSMR-CH10), proinsulin (Alpco #80-PINMS-E01), C-peptide (Alpco #80-CPTMS-E01), glucagon (Mercodia, #10-1281-01). Measurements were performed on a Spark plate reader (TECAN), and analysed using (GraphPad Software Inc., San Diego, CA).

Mathematical modeling

We used a modified version of the Topp model (Topp et al., 2000) to simulate glucose and insulin dynamics (see equations in Fig. 6A). Parameter values for the glucose and insulin equations were modified by hand so that the model matched a typical wildtype female low-fat-diet glucose tolerance test time series and predicted the observed beta cell mass in these mice. We included an inhibition factor, $1/(1 + S_\beta I)$, multiplying the insulin secretion term that accounts for insulin receptor-mediated negative feedback on insulin secretion, parametrized by S_β , β -cell Insr-specific insulin sensitivity. In glucose clamp conditions, a simple equation relates S_β to steady state insulin levels in wildtype and mutant mice: $S_\beta = (I_m^* - I_{wt}^*) / (I_m^*)^2$, where I_{wt}^* is the steady state insulin level for wild type control mice, and I_m^* is the equivalent for the β /InsrKO mice. We assumed that, at each time point after the first one in the glucose-clamp insulin measurements, the blood insulin levels were hovering around steady

state and all other parameters and variables were constant (Fig. S5A). We used those steady state data points to estimate S_β for the male and female wild type mice using this equation.

Glucose tolerance tests were simulated for various S_β and S_P values by calculating the IG system steady state values for each S_β and S_P , then using the steady state value as the initial condition for insulin, and steady state plus 20 mM as the initial condition for glucose. Fig. 6A shows sample in silico glucose tolerance tests for various values of S_β , with S_P fixed at 70. The glucose tolerance area under the glucose curve (AUGC) was then calculated for each set of S_β and S_P , generating a numerical map from S_β and S_P to AUGC. From the glucose tolerance tests in wildtype and mutant male mice and wildtype and mutant female mice, we calculated the experimental AUGC values at 4, 9, 21 and 39 weeks. Using the computed AUGC map and the S_β values calculated from the glucose-clamp data, we estimated the S_P value that would give the experimental AUGC (Fig. S5C)

Statistics

Data are presented as mean +/- SEM, with individual data points, unless otherwise indicated. T-tests were performed when only 2 groups were compared at a single timepoint. One-way ANOVA was applied when three groups were compared at a single timepoint. Mixed effects model statistics were used for statistical analysis of GTT, ITT, GSIS experiments. Specifically, a fitted mixed model (Prism 8, Graph Pad), which allows for missing measurements and un-even group sizes, was applied when 2 or more groups were compared at multiple time points (e.g. 4h fasted blood glucose, insulin, proinsulin, c-peptide and body weight).

References

1. Alejandro, E.U., Kalynyak, T.B., Taghizadeh, F., Gwiazda, K.S., Rawstron, E.K., Jacob, K.J., and Johnson, J.D. (2010). Acute insulin signaling in pancreatic beta-cells is mediated by multiple Raf-1 dependent pathways. *Endocrinology* 151, 502-512.
2. Alonso, L.C., Yokoe, T., Zhang, P., Scott, D.K., Kim, S.K., O'Donnell, C.P., and Garcia-Ocana, A. (2007). Glucose infusion in mice: a new model to induce beta-cell replication. *Diabetes* 56, 1792-1801.
3. Anderson, K.R., Singer, R.A., Balderes, D.A., Hernandez-Lagunas, L., Johnson, C.W., Artinger, K.B., and Sussel, L. (2011). The L6 domain tetraspanin Tm4sf4 regulates endocrine pancreas differentiation and directed cell migration. *Development* 138, 3213-3224.
4. Ashok, A., and Singh, N. (2018). Prion protein modulates glucose homeostasis by altering intracellular iron. *Sci Rep* 8, 6556.
5. Aspinwall, C.A., Lakey, J.R., and Kennedy, R.T. (1999). Insulin-stimulated insulin secretion in single pancreatic beta cells. *J Biol Chem* 274, 6360-6365.
6. Beith, J.L., Alejandro, E.U., and Johnson, J.D. (2008). Insulin stimulates primary beta-cell proliferation via Raf-1 kinase. *Endocrinology* 149, 2251-2260.
7. Bernal-Mizrachi, E., Fatrai, S., Johnson, J.D., Ohsugi, M., Otani, K., Han, Z., Polonsky, K.S., and Permutt, M.A. (2004). Defective insulin secretion and increased susceptibility to experimental diabetes are induced by reduced Akt activity in pancreatic islet beta cells. *J Clin Invest* 114, 928-936.
8. Boothe, T., Lim, G.E., Cen, H., Skovso, S., Piske, M., Li, S.N., Nabi, I.R., Gilon, P., and Johnson, J.D. (2016). Inter-domain tagging implicates caveolin-1 in insulin receptor trafficking and Erk signaling bias in pancreatic beta-cells. *Mol Metab* 5, 366-378.
9. Bouche, C., Lopez, X., Fleischman, A., Cypess, A.M., O'Shea, S., Stefanovski, D., Bergman, R.N., Rogatsky, E., Stein, D.T., Kahn, C.R., et al. (2010). Insulin enhances glucose-stimulated insulin secretion in healthy humans. *Proc Natl Acad Sci U S A* 107, 4770-4775.
10. Boucher, J., Kleinridders, A., and Kahn, C.R. (2014). Insulin receptor signaling in normal and insulin-resistant states. *Cold Spring Harb Perspect Biol* 6.
11. Braun, M., Ramracheya, R., and Rorsman, P. (2012). Autocrine regulation of insulin secretion. *Diabetes, Obesity and Metabolism* 14, 143-151.

12. Cavallo-Perin, P., Bruno, A., Scaglione, L., Gruden, G., Cassader, M., and Pagano, G. (1993). Feedback inhibition of insulin and glucagon secretion by insulin is altered in abdominal obesity with normal or impaired glucose tolerance. *Acta Diabetol* 30, 154-158.
13. Chamberlain, C.E., Scheel, D.W., McGlynn, K., Kim, H., Miyatsuka, T., Wang, J., Nguyen, V., Zhao, S., Mavropoulos, A., Abraham, A.G., et al. (2014). Menin determines K-RAS proliferative outputs in endocrine cells. *J Clin Invest* 124, 4093-4101.
14. Dai, F.F., Bhattacharjee, A., Liu, Y., Batchuluun, B., Zhang, M., Wang, X.S., Huang, X., Luu, L., Zhu, D., Gaisano, H., et al. (2015). A Novel GLP1 Receptor Interacting Protein ATP6ap2 Regulates Insulin Secretion in Pancreatic Beta Cells. *J Biol Chem* 290, 25045-25061.
15. Elahi, D., Nagulesparan, M., Hershcopf, R.J., Muller, D.C., Tobin, J.D., Blix, P.M., Rubenstein, A.H., Unger, R.H., and Andres, R. (1982). Feedback inhibition of insulin secretion by insulin: relation to the hyperinsulinemia of obesity. *N Engl J Med* 306, 1196-1202.
16. Engin, F., Yermalovich, A., Nguyen, T., Hummasti, S., Fu, W., Eizirik, D.L., Mathis, D., and Hotamisligil, G.S. (2013). Restoration of the unfolded protein response in pancreatic beta cells protects mice against type 1 diabetes. *Sci Transl Med* 5, 211ra156.
17. Esser, N., Utzschneider, K.M., and Kahn, S.E. (2020). Early beta cell dysfunction vs insulin hypersecretion as the primary event in the pathogenesis of dysglycaemia. *Diabetologia* 63, 2007-2021.
18. Fan, Y., Rudert, W.A., Grupillo, M., He, J., Sisino, G., and Trucco, M. (2009). Thymus-specific deletion of insulin induces autoimmune diabetes. *The EMBO journal* 28, 2812-2824.
19. Fisher, S.J., Bruning, J.C., Lannon, S., and Kahn, C.R. (2005). Insulin signaling in the central nervous system is critical for the normal sympathoadrenal response to hypoglycemia. *Diabetes* 54, 1447-1451.
20. Fornoni, A., Pileggi, A., Molano, R.D., Sanabria, N.Y., Tejada, T., Gonzalez-Quintana, J., Ichii, H., Inverardi, L., Ricordi, C., and Pastori, R.L. (2008). Inhibition of c-jun N terminal kinase (JNK) improves functional beta cell mass in human islets and leads to AKT and glycogen synthase kinase-3 (GSK-3) phosphorylation. *Diabetologia* 51, 298-308.
21. Frau, F., Crowther, D., Ruettens, H., and Allebrandt, K.V. (2017). Type-2 diabetes-associated variants with cross-trait relevance: Post-GWAs strategies for biological function interpretation. *Mol Genet Metab* 121, 43-50.
22. Gomez-Banoy, N., Guseh, J.S., Li, G., Rubio-Navarro, A., Chen, T., Poirier, B., Putzel, G., Rosselot, C., Pabon, M.A., Camporez, J.P., et al. (2019). Adipsin preserves beta cells in diabetic mice and associates with protection from type 2 diabetes in humans. *Nat Med* 25, 1739-1747.
23. Gopel, S.O., Kanno, T., Barg, S., Weng, X.G., Gromada, J., and Rorsman, P. (2000). Regulation of glucagon release in mouse -cells by KATP channels and inactivation of TTX-sensitive Na⁺ channels. *J Physiol* 528, 509-520.
24. Goulley, J., Dahl, U., Baeza, N., Mishina, Y., and Edlund, H. (2007). BMP4-BMPR1A signaling in beta cells is required for and augments glucose-stimulated insulin secretion. *Cell Metab* 5, 207-219.
25. Gu, H., Do, D.V., Liu, X., Xu, L., Su, Y., Nah, J.M., Wong, Y., Li, Y., Sheng, N., Tilaye, G.A., et al. (2018). The STAT3 Target Mettl8 Regulates Mouse ESC Differentiation via Inhibiting the JNK Pathway. *Stem Cell Reports* 10, 1807-1820.
26. Gunton, J.E., Kulkarni, R.N., Yim, S., Okada, T., Hawthorne, W.J., Tseng, Y.H., Roberson, R.S., Ricordi, C., O'Connell P, J., Gonzalez, F.J., et al. (2005). Loss of ARNT/HIF1beta Mediates Altered Gene Expression and Pancreatic-Islet Dysfunction in Human Type 2 Diabetes. *Cell* 122, 337-349.
27. Hafemeister, C., and Satija, R. (2019). Normalization and variance stabilization of single-cell RNA-seq data using regularized negative binomial regression. *Genome Biol* 20, 296.
28. Hara, M., Wang, X., Paz, V.P., Cox, N.J., Iwasaki, N., Ogata, M., Iwamoto, Y., and Bell, G.I. (2000). No diabetes-associated mutations in the coding region of the hepatocyte nuclear factor-4gamma gene (HNF4G) in Japanese patients with MODY. *Diabetologia* 43, 1064-1069.
29. Iversen, J., and Miles, D.W. (1971). Evidence for a Feedback Inhibition of Insulin on Insulin Secretion in the Isolated, Perfused Canine Pancreas. *Diabetes* 20, 1-9.

30. Jhala, U.S., Canettieri, G., Sreaton, R.A., Kulkarni, R.N., Krajewski, S., Reed, J., Walker, J., Lin, X., White, M., and Montminy, M. (2003). cAMP promotes pancreatic beta-cell survival via CREB-mediated induction of IRS2. *Genes Dev* 17, 1575-1580.
31. Johnson, J.D. (2014). A practical guide to genetic engineering of pancreatic beta-cells in vivo: getting a grip on RIP and MIP. *Islets* 6, e944439.
32. Johnson, J.D., Bernal-Mizrachi, E., Alejandro, E.U., Han, Z., Kalynyak, T.B., Li, H., Beith, J.L., Gross, J., Warnock, G.L., Townsend, R.R., et al. (2006a). Insulin protects islets from apoptosis via Pdx1 and specific changes in the human islet proteome. *Proc Natl Acad Sci U S A* 103, 19575-19580.
33. Johnson, J.D., Ford, E.L., Bernal-Mizrachi, E., Kusser, K.L., Luciani, D.S., Han, Z., Tran, H., Randall, T.D., Lund, F.E., and Polonsky, K.S. (2006b). Suppressed Insulin Signaling and Increased Apoptosis in Cd38-Null Islets. *Diabetes* 55, 2737-2746.
34. Johnson, J.D., and Misler, S. (2002a). Nicotinic acid-adenine dinucleotide phosphate-sensitive calcium stores initiate insulin signaling in human beta cells. *Proc Natl Acad Sci U S A* 99, 14566-14571.
35. Johnson, J.D., and Misler, S. (2002b). Nicotinic acid-adenine dinucleotide phosphate-sensitive calcium stores initiate insulin signaling in human beta cells. *Proceedings of the National Academy of Sciences* 99, 14566-14571.
36. Khan, F.A., Goforth, P.B., Zhang, M., and Satin, L.S. (2001). Insulin activates ATP-sensitive K(+) channels in pancreatic beta-cells through a phosphatidylinositol 3-kinase-dependent pathway. *Diabetes* 50, 2192-2198.
37. Kido, Y., Burks, D.J., Withers, D., Bruning, J.C., Kahn, C.R., White, M.F., and Accili, D. (2000). Tissue-specific insulin resistance in mice with mutations in the insulin receptor, IRS-1, and IRS-2. *J Clin Invest* 105, 199-205.
38. Kline, C.F., Wright, P.J., Koval, O.M., Zmuda, E.J., Johnson, B.L., Anderson, M.E., Hai, T., Hund, T.J., and Mohler, P.J. (2013). betalV-Spectrin and CaMKII facilitate Kir6.2 regulation in pancreatic beta cells. *Proc Natl Acad Sci U S A* 110, 17576-17581.
39. Knutson, V.P., Ronnett, G.V., and Lane, M.D. (1983). Rapid, reversible internalization of cell surface insulin receptors. Correlation with insulin-induced down-regulation. *J Biol Chem* 258, 12139-12142.
40. Kolic, J., Manning Fox, J.E., Chepurny, O.G., Spigelman, A.F., Ferdaoussi, M., Schwede, F., Holz, G.G., and MacDonald, P.E. (2016). PI3 kinases p110alpha and PI3K-C2beta negatively regulate cAMP via PDE3/8 to control insulin secretion in mouse and human islets. *Mol Metab* 5, 459-471.
41. Konner, A.C., Janoschek, R., Plum, L., Jordan, S.D., Rother, E., Ma, X., Xu, C., Enriori, P., Hampel, B., Barsh, G.S., et al. (2007). Insulin action in AgRP-expressing neurons is required for suppression of hepatic glucose production. *Cell Metab* 5, 438-449.
42. Kulkarni, R.N., Bruning, J.C., Winnay, J.N., Postic, C., Magnuson, M.A., and Kahn, C.R. (1999). Tissue-specific knockout of the insulin receptor in pancreatic beta cells creates an insulin secretory defect similar to that in type 2 diabetes. *Cell* 96, 329-339.
43. Laraia, L., Friese, A., Corkery, D.P., Konstantinidis, G., Erwin, N., Hofer, W., Karatas, H., Klewer, L., Brockmeyer, A., Metz, M., et al. (2019). The cholesterol transfer protein GRAMD1A regulates autophagosome biogenesis. *Nat Chem Biol* 15, 710-720.
44. Leibiger, I.B., Leibiger, B., and Berggren, P.-O. (2008). Insulin Signaling in the Pancreatic β -Cell. *Annual Review of Nutrition* 28, 233-251.
45. Locke, J.M., Hysenaj, G., Wood, A.R., Weedon, M.N., and Harries, L.W. (2015). Targeted allelic expression profiling in human islets identifies cis-regulatory effects for multiple variants identified by type 2 diabetes genome-wide association studies. *Diabetes* 64, 1484-1491.
46. Luciani, D.S., and Johnson, J.D. (2005). Acute effects of insulin on beta-cells from transplantable human islets. *Mol Cell Endocrinol* 241, 88-98.
47. Ma, F., Zhang, C., Prasad, K.V., Freeman, G.J., and Schlossman, S.F. (2001). Molecular cloning of Porimin, a novel cell surface receptor mediating oncotic cell death. *Proc Natl Acad Sci U S A* 98, 9778-9783.

48. Ma, X., Zhang, Y., Gromada, J., Sewing, S., Berggren, P.-O., Buschard, K., Salehi, A., Vikman, J., Rorsman, P., and Eliasson, L. (2005). Glucagon Stimulates Exocytosis in Mouse and Rat Pancreatic α -Cells by Binding to Glucagon Receptors. *Molecular Endocrinology* 19, 198-212.
49. Mandrup-Poulsen, T. (2003). Apoptotic signal transduction pathways in diabetes. *Biochem Pharmacol* 66, 1433-1440.
50. Mari, A., Tura, A., Natali, A., Anderwald, C., Balkau, B., Lalic, N., Walker, M., Ferrannini, E., and Investigators, R. (2011). Influence of hyperinsulinemia and insulin resistance on in vivo beta-cell function: their role in human beta-cell dysfunction. *Diabetes* 60, 3141-3147.
51. Mauvais-Jarvis, F. (2015). Sex differences in metabolic homeostasis, diabetes, and obesity. *Biol Sex Differ* 6, 14.
52. Mehran, A.E., Templeman, N.M., Brigidi, G.S., Lim, G.E., Chu, K.Y., Hu, X., Botezelli, J.D., Asadi, A., Hoffman, B.G., Kieffer, T.J., et al. (2012). Hyperinsulinemia drives diet-induced obesity independently of brain insulin production. *Cell Metab* 16, 723-737.
53. Mokhtari, D., Barbu, A., Mehmeti, I., Vercamer, C., and Welsh, N. (2009). Overexpression of the nuclear factor-kappaB subunit c-Rel protects against human islet cell death in vitro. *Am J Physiol Endocrinol Metab* 297, E1067-1077.
54. Mosleh, E., Ou, K., Haemmerle, M.W., Tembo, T., Yuhas, A., Carboneau, B.A., Townsend, S.E., Bosma, K.J., Gannon, M., O'Brien, R.M., et al. (2020). Ins1-Cre and Ins1-CreER Gene Replacement Alleles Are Susceptible To Silencing By DNA Hypermethylation. *Endocrinology* 161.
55. Muller, D., Jones, P.M., and Persaud, S.J. (2006). Autocrine anti-apoptotic and proliferative effects of insulin in pancreatic beta-cells. *Febs Letters* 580, 6977-6980.
56. Nicholson, A., Reifsnyder, P.C., Malcolm, R.D., Lucas, C.A., MacGregor, G.R., Zhang, W., and Leiter, E.H. (2010). Diet-induced obesity in two C57BL/6 substrains with intact or mutant nicotinamide nucleotide transhydrogenase (Nnt) gene. *Obesity (Silver Spring)* 18, 1902-1905.
57. Norman, A.W., and Henry, H.L. (2014). Hormones. Academic Press.
58. Oakie, A., Zhou, L., Rivers, S., Cheung, C., Li, J., and Wang, R. (2020). Postnatal knockout of beta cell insulin receptor impaired insulin secretion in male mice exposed to high-fat diet stress. *Mol Cell Endocrinol* 499, 110588.
59. Ohsugi, M., Cras-Meneur, C., Zhou, Y., Bernal-Mizrachi, E., Johnson, J.D., Luciani, D.S., Polonsky, K.S., and Permutt, M.A. (2005). Reduced expression of the insulin receptor in mouse insulinoma (MIN6) cells reveals multiple roles of insulin signaling in gene expression, proliferation, insulin content, and secretion. *Journal of Biological Chemistry* 280, 4992-5003.
60. Okada, T., Liew, C.W., Hu, J., Hinault, C., Michael, M.D., Krutzfeldt, J., Yin, C., Holzenberger, M., Stoffel, M., and Kulkarni, R.N. (2007). Insulin receptors in beta-cells are critical for islet compensatory growth response to insulin resistance. *Proc Natl Acad Sci U S A* 104, 8977-8982.
61. Okamoto, H., Nakae, J., Kitamura, T., Park, B.C., Dragatsis, I., and Accili, D. (2004). Transgenic rescue of insulin receptor-deficient mice. *J Clin Invest* 114, 214-223.
62. Oropeza, D., Jouvet, N., Budry, L., Campbell, J.E., Bouyakdan, K., Lacombe, J., Perron, G., Bergeron, V., Neuman, J.C., Brar, H.K., et al. (2015). Phenotypic Characterization of MIP-CreERT1Lphi Mice With Transgene-Driven Islet Expression of Human Growth Hormone. *Diabetes* 64, 3798-3807.
63. Otani, K., Kulkarni, R.N., Baldwin, A.C., Krutzfeldt, J., Ueki, K., Stoffel, M., Kahn, C.R., and Polonsky, K.S. (2003). Reduced β -cell mass and altered glucose sensing impairs insulin secretory function in mice with pancreatic β -cell knockout of the insulin receptor. *Am J Physiol Endocrinol Metab*.
64. Otani, K., Kulkarni, R.N., Baldwin, A.C., Krutzfeldt, J., Ueki, K., Stoffel, M., Kahn, C.R., and Polonsky, K.S. (2004). Reduced beta-cell mass and altered glucose sensing impair insulin-secretory function in betalRKO mice. *Am J Physiol Endocrinol Metab* 286, E41-49.
65. Page, M.M., and Johnson, J.D. (2018). Mild Suppression of Hyperinsulinemia to Treat Obesity and Insulin Resistance. *Trends Endocrinol Metab* 29, 389-399.
66. Parks, B.W., Sallam, T., Mehrabian, M., Psychogios, N., Hui, S.T., Norheim, F., Castellani, L.W., Rau, C.D., Pan, C., Phun, J., et al. (2015). Genetic architecture of insulin resistance in the mouse. *Cell Metab* 21, 334-347.

67. Paschen, M., Moede, T., Valladolid-Acebes, I., Leibiger, B., Moruzzi, N., Jacob, S., Garcia-Prieto, C.F., Brismar, K., Leibiger, I.B., and Berggren, P.O. (2019). Diet-induced beta-cell insulin resistance results in reversible loss of functional beta-cell mass. *Faseb J* 33, 204-218.
68. Picelli, S., Faridani, O.R., Bjorklund, A.K., Winberg, G., Sagasser, S., and Sandberg, R. (2014). Full-length RNA-seq from single cells using Smart-seq2. *Nat Protoc* 9, 171-181.
69. Plum, L., Schubert, M., and Bruning, J.C. (2005). The role of insulin receptor signaling in the brain. *Trends Endocrinol Metab* 16, 59-65.
70. Prentki, M., and Nolan, C.J. (2006). Islet beta cell failure in type 2 diabetes. *J Clin Invest* 116, 1802-1812.
71. Prigge, J.R., Wiley, J.A., Talago, E.A., Young, E.M., Johns, L.L., Kundert, J.A., Sonsteng, K.M., Halford, W.P., Capecchi, M.R., and Schmidt, E.E. (2013). Nuclear double-fluorescent reporter for in vivo and ex vivo analyses of biological transitions in mouse nuclei. *Mamm Genome*.
72. Rappaport, A.M., Ohira, S., Coddling, J.A., Empey, G., Kalnins, A., Lin, B.J., and Haist, R.E. (1972). Effects on insulin output and on pancreatic blood flow of exogenous insulin infusion into an in situ isolated portion of the pancreas. *Endocrinology* 91, 168-176.
73. Rorsman, P., and Ashcroft, F.M. (2018). Pancreatic β -Cell Electrical Activity and Insulin Secretion: Of Mice and Men. *Physiological Reviews* 98, 117-214.
74. Salvalaggio, P.R., Deng, S., Ariyan, C.E., Millet, I., Zawalich, W.S., Basadonna, G.P., and Rothstein, D.M. (2002). Islet filtration: a simple and rapid new purification procedure that avoids ficoll and improves islet mass and function. *Transplantation* 74, 877-879.
75. Schmidt, T., Samaras, P., Frejno, M., Gessulat, S., Barnert, M., Kienegger, H., Krcmar, H., Schlegl, J., Ehrlich, H.C., Aiche, S., et al. (2018). ProteomicsDB. *Nucleic Acids Res* 46, D1271-D1281.
76. Sharma, R.B., O'Donnell, A.C., Stamateris, R.E., Ha, B., McCloskey, K.M., Reynolds, P.R., Arvan, P., and Alonso, L.C. (2015). Insulin demand regulates beta cell number via the unfolded protein response. *J Clin Invest* 125, 3831-3846.
77. Stamateris, R.E., Sharma, R.B., Kong, Y., Ebrahimpour, P., Panday, D., Ranganath, P., Zou, B., Levitt, H., Parambil, N.A., O'Donnell, C.P., et al. (2016). Glucose Induces Mouse beta-Cell Proliferation via IRS2, MTOR, and Cyclin D2 but Not the Insulin Receptor. *Diabetes* 65, 981-995.
78. Stancill, J.S., Osipovich, A.B., Cartailler, J.P., and Magnuson, M.A. (2019). Transgene-associated human growth hormone expression in pancreatic beta-cells impairs identification of sex-based gene expression differences. *Am J Physiol Endocrinol Metab* 316, E196-E209.
79. Strawbridge, R.J., Dupuis, J., Prokopenko, I., Barker, A., Ahlvist, E., Rybin, D., Petrie, J.R., Travers, M.E., Bouatia-Naji, N., Dimas, A.S., et al. (2011). Genome-wide association identifies nine common variants associated with fasting proinsulin levels and provides new insights into the pathophysiology of type 2 diabetes. *Diabetes* 60, 2624-2634.
80. Stuart, T., Butler, A., Hoffman, P., Hafemeister, C., Papalex, E., Mauck, W.M., 3rd, Hao, Y., Stoeckius, M., Smibert, P., and Satija, R. (2019). Comprehensive Integration of Single-Cell Data. *Cell* 177, 1888-1902 e1821.
81. Tabak, A.G., Herder, C., Rathmann, W., Brunner, E.J., and Kivimaki, M. (2012). Prediabetes: a high-risk state for diabetes development. *Lancet* 379, 2279-2290.
82. Templeman, N.M., Clee, S.M., and Johnson, J.D. (2015). Suppression of hyperinsulinaemia in growing female mice provides long-term protection against obesity. *Diabetologia*.
83. Templeman, N.M., Flibotte, S., Chik, J.H.L., Sinha, S., Lim, G.E., Foster, L.J., Nislow, C., and Johnson, J.D. (2017). Reduced Circulating Insulin Enhances Insulin Sensitivity in Old Mice and Extends Lifespan. *Cell Rep* 20, 451-463.
84. Thorens, B., Tarussio, D., Maestro, M.A., Rovira, M., Heikkila, E., and Ferrer, J. (2015). Ins1(Cre) knock-in mice for beta cell-specific gene recombination. *Diabetologia* 58, 558-565.
85. Tobi, E.W., Slieker, R.C., Luijk, R., Dekkers, K.F., Stein, A.D., Xu, K.M., Biobank-based Integrative Omics Studies, C., Slagboom, P.E., van Zwet, E.W., Lumey, L.H., et al. (2018). DNA methylation as a mediator of the association between prenatal adversity and risk factors for metabolic disease in adulthood. *Sci Adv* 4, eaao4364.

86. Topp, B., Promislow, K., deVries, G., Miura, R.M., and Finegood, D.T. (2000). A model of beta-cell mass, insulin, and glucose kinetics: pathways to diabetes. *J Theor Biol* 206, 605-619.
87. Vogt, M.C., and Bruning, J.C. (2013). CNS insulin signaling in the control of energy homeostasis and glucose metabolism - from embryo to old age. *Trends Endocrinol Metab* 24, 76-84.
88. Wang, F., Pulinilkunnil, T., Flibotte, S., Nislow, C., Vlodavsky, I., Hussein, B., and Rodrigues, B. (2019). Heparanase protects the heart against chemical or ischemia/reperfusion injury. *J Mol Cell Cardiol* 131, 29-40.
89. Wang, J., Gu, W., and Chen, C. (2018). Knocking down Insulin Receptor in Pancreatic Beta Cell lines with Lentiviral-Small Hairpin RNA Reduces Glucose-Stimulated Insulin Secretion via Decreasing the Gene Expression of Insulin, GLUT2 and Pdx1. *International journal of molecular sciences* 19.
90. Wang, M., Li, J., Lim, G.E., and Johnson, J.D. (2013). Is dynamic autocrine insulin signaling possible? A mathematical model predicts picomolar concentrations of extracellular monomeric insulin within human pancreatic islets. *PloS one* 8, e64860.
91. Wang, Z., Ramanadham, S., Ma, Z.A., Bao, S., Mancuso, D.J., Gross, R.W., and Turk, J. (2005). Group VIA phospholipase A2 forms a signaling complex with the calcium/calmodulin-dependent protein kinase IIbeta expressed in pancreatic islet beta-cells. *J Biol Chem* 280, 6840-6849.
92. Wicksteed, B., Brissova, M., Yan, W., Opland, D.M., Plank, J.L., Reinert, R.B., Dickson, L.M., Tamarina, N.A., Philipson, L.H., Shostak, A., et al. (2010a). Conditional gene targeting in mouse pancreatic beta-cells: analysis of ectopic Cre transgene expression in the brain. *Diabetes* 59, 3090-3098.
93. Wicksteed, B., Brissova, M., Yan, W., Opland, D.M., Plank, J.L., Reinert, R.B., Dickson, L.M., Tamarina, N.A., Philipson, L.H., Shostak, A., et al. (2010b). Conditional gene targeting in mouse pancreatic ss-Cells: analysis of ectopic Cre transgene expression in the brain. *Diabetes* 59, 3090-3098.
94. Wills, Q.F., Boothe, T., Asadi, A., Ao, Z., Warnock, G.L., Kieffer, T.J., and Johnson, J.D. (2016). Statistical approaches and software for clustering islet cell functional heterogeneity. *Islets* 8, 48-56.
95. Yaekura, K., Julyan, R., Wicksteed, B.L., Hays, L.B., Alarcon, C., Sommers, S., Poitout, V., Baskin, D.G., Wang, Y., Philipson, L.H., et al. (2003). Insulin secretory deficiency and glucose intolerance in Rab3A null mice. *J Biol Chem* 278, 9715-9721.
96. Yang, Y.H., Wills, Q.F., and Johnson, J.D. (2015). A live-cell, high-content imaging survey of 206 endogenous factors across five stress conditions reveals context-dependent survival effects in mouse primary beta cells. *Diabetologia* 58, 1239-1249.
97. Yki-Jarvinen, H. (1984). Sex and insulin sensitivity. *Metabolism* 33, 1011-1015.
98. Zhang, A.M.Y., Magrill, J., de Winter, T.J.J., Hu, X., Skovso, S., Schaeffer, D.F., Kopp, J.L., and Johnson, J.D. (2019). Endogenous Hyperinsulinemia Contributes to Pancreatic Cancer Development. *Cell Metab* 30, 403-404.
99. Zhang, B., Chang, A., Kjeldsen, T.B., and Arvan, P. (2001). Intracellular retention of newly synthesized insulin in yeast is caused by endoproteolytic processing in the Golgi complex. *J Cell Biol* 153, 1187-1198.
100. Zhang, F., Zhang, Q., Tengholm, A., and Sjoholm, A. (2006). Involvement of JAK2 and Src kinase tyrosine phosphorylation in human growth hormone-stimulated increases in cytosolic free Ca²⁺ and insulin secretion. *Am J Physiol Cell Physiol* 291, C466-475.
101. Zhang, Z., Zhang, W., Jung, D.Y., Ko, H.J., Lee, Y., Friedline, R.H., Lee, E., Jun, J., Ma, Z., Kim, F., et al. (2012). TRPM2 Ca²⁺ channel regulates energy balance and glucose metabolism. *American journal of physiology. Endocrinology and metabolism* 302, E807-816.
102. Zhou, G., Soufan, O., Ewald, J., Hancock, R.E.W., Basu, N., and Xia, J. (2019). NetworkAnalyst 3.0: a visual analytics platform for comprehensive gene expression profiling and meta-analysis. *Nucleic Acids Res* 47, W234-W241.

Figure Legends

Figure 1. An animal model to examine the role of abundant Insr in β -cells. **(A)** INSR protein (isoform A and B) and *INSR* mRNA expression across human tissues. *Left 3 columns* show INSR isoform A and B protein abundance expressed as normalized median intensity (NMI; www.proteomicsdb.org). *Right 3 columns* show total *INSR* mRNA expression in the same tissues (where available) extracted from 3 databases. *Left to right*, mRNA data from human proteome atlas (HPA) and genotype tissue expression project (GTEX) are shown in reads per kilobase million (RPKM). Data from the FAMTOMS database is shown as transcripts per kilobase million (TMP). **(B)** Human insulin receptor expression in islet cell subtypes extracted from an integrated dataset of human single cell RNA seq data (see Methods). Normalized expression levels are shown in UMAP space (*top*) and as a ridge plot on a log scale (*bottom*). The height of the ridge indicates the frequency of cells at a given expression level. **(C)** Breeding strategy for generating β -cell specific $\beta/Insr^{KO}$, ($\beta/Insr^{HET}$), and littermate control Cre-only mice. **(D)** Robust Cre recombination verified by imaging the nTnG reporter allele in an isolated islet from an *Insl1^{Cre/wt},nTnG* mouse. **(E)** Western blot of Insr protein in islets isolated from $\beta/Insr^{KO}$, ($\beta/Insr^{HET}$), and littermate control Cre-only mice. **(F)** *Insr* mRNA expression across tissues in 16 week-old LFD-fed control, $\beta/Insr^{HET}$, and $\beta/Insr^{KO}$ mice assessed by qPCR (n=3 in females, n=5-6 in males).

Figure 2. Transcriptomic analysis of purified *Insr* deficient β -cells. **(A)** Differentially expressed genes between FACS purified GFP-positive β -cells from $\beta/Insr^{KO}$ and control mice are shown overlaid on a diagram of their predicted functional roles. See Figure S1 for full gene names.

Figure 3. β -Cells lacking *Insr* have increased action potential and calcium oscillation frequencies. **(A,B)** Representative image and quantification of Slc2a2 (Glut2) in islet from sectioned pancreas from a LFD-fed 13 week old female control and $\beta/Insr^{KO}$ mice. Unpaired t-test. **(C)** Oxygen consumption rate data of dispersed islets from 16 week-old chow-fed control, $\beta/Insr^{HET}$, and $\beta/Insr^{KO}$ mice. Data analyzed with mixed effects model from independent islet cultures from 3 male and 1 female mice. **(D)** Representative traces of action potential firing in β -cells from 16 week-old chow-fed mice. Glucose changed as indicated. **(E-G)** Quantification of action potential properties and reversal potential during the 10mM glucose phase in patch clamped dispersed β -cells. Data analyzed using unpaired t-test (n=16-17 cells, from 3 mice per group). **(H)** β -Cell exocytosis measured as increased membrane capacitance normalized to initial cell size (fF/pF) over a series of ten 500 ms membrane depolarizations from -70 to 0 mV (n= control 32 cells, 29 $\beta/Insr^{KO}$ cells, from 3 pairs of mice). **(I)** Ca^{2+} dynamics measured in dispersed islet cells (Fura-2 340/380 ratio) treated as indicated from a baseline of 3 mM glucose. **(J)** Quantification of glucose induced Ca^{2+} oscillation number (n=3523 cells). ANOVA with correction for multiple comparisons using Tukey's method. Additional quantification of these traces can be found in Fig. S2.

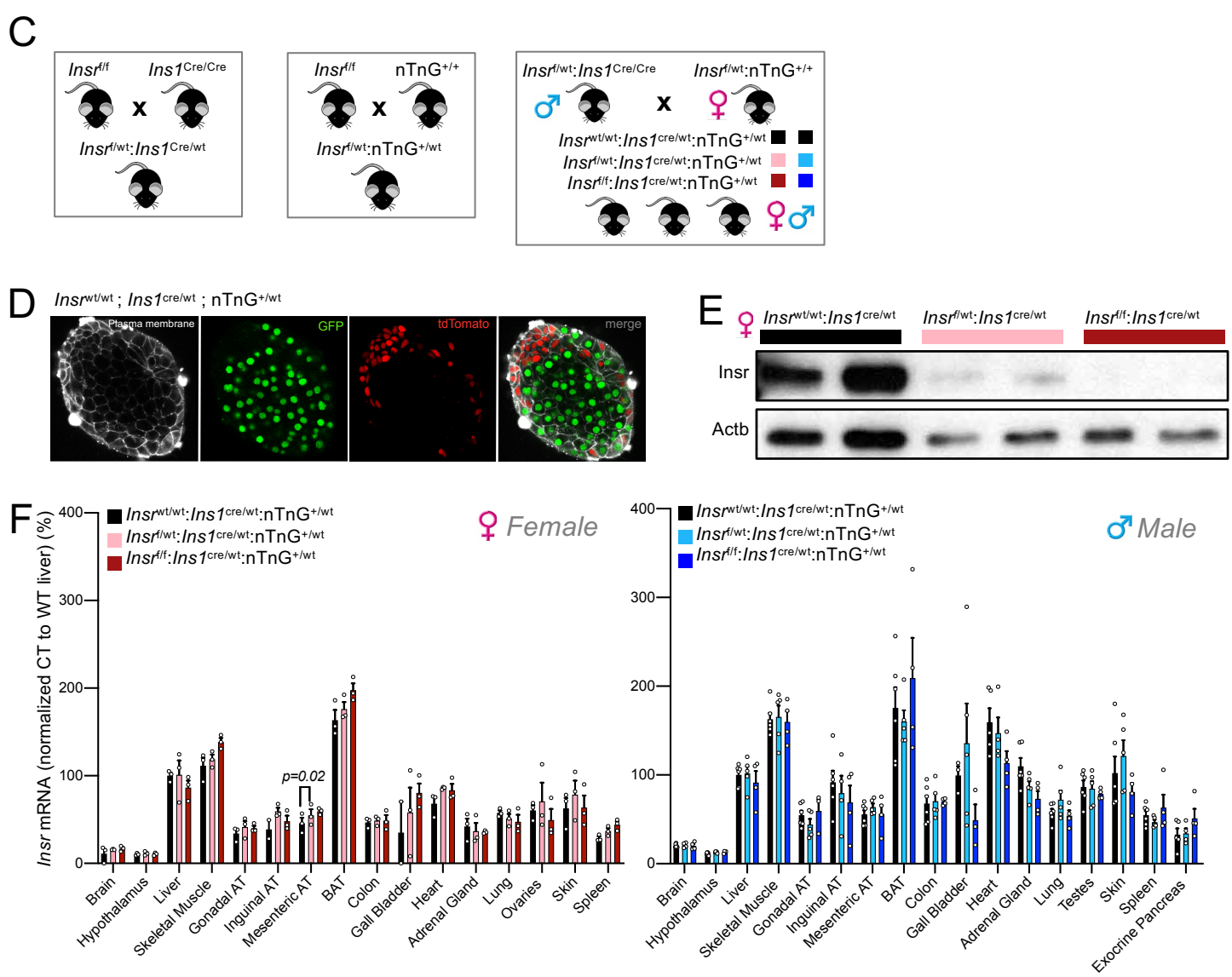
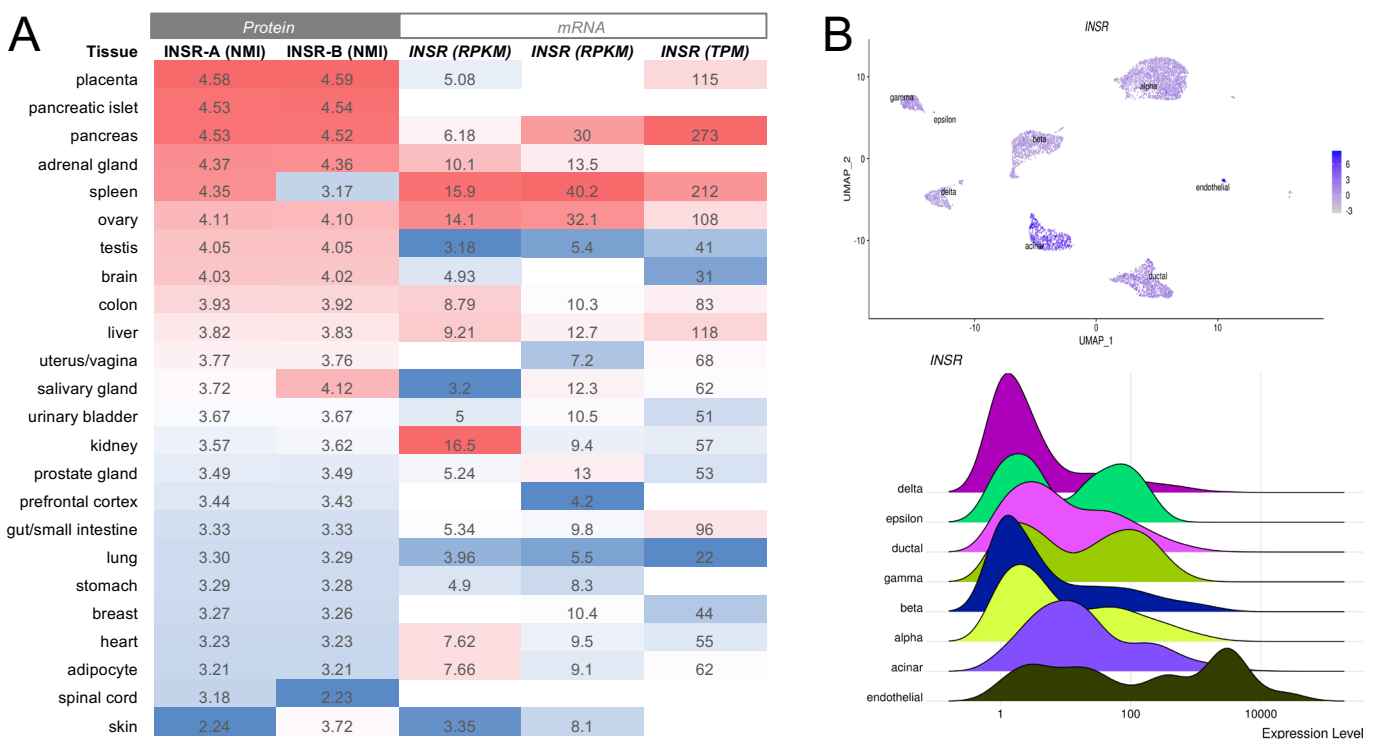
Figure 4. *Insr* knockout increases glucose-stimulated insulin secretion *in vitro* and *in vivo*. **(A,B)** Perifused islets isolated from 16 week old chow-fed control, $\beta/Insr^{HET}$, $\beta/Insr^{KO}$ **(A)** female (n=3,3,5), and **(B)** male (n=6,5,5) mice were exposed to 20 mM glucose (20G), 10 mM glucose (10G),

and 30 mM KCL (KCL) from a baseline of 3 mM glucose. Data analyzed using repeated measures mixed effects model. Quantification of area under the curve (AUC) is shown for 1st phase and 2nd phase during 15 mM glucose stimulation, total response during 10 mM glucose stimulation, and during 30mM KCL stimulation. AUC's were analyzed with 1-way ANOVA analysis. **(C,F)** Glucose infusion rates, **(D,G)** plasma glucose levels, and **(E,H)** plasma insulin levels during 2 h hyperglycemic clamps in awake of LFD-fed 10 week old LFD-fed control and $\beta\text{Insr}^{\text{KO}}$ female (n=14, 15) and male (n=4, 4) mice. Data were analyzed using repeated measures mixed effects model. **(I,J)** Insulin levels (% basal insulin) following a single glucose injection (2g glucose/kg body mass, *i.p.*) of 11 week old LFD-fed control, $\beta\text{Insr}^{\text{HET}}$, $\beta\text{Insr}^{\text{KO}}$ female (n=33,34,23) and male (n=22,29,17) mice. Data were analyzed using repeated measures mixed effects model. **(K,L)** 30min islet protein synthesis measured by S35 labeling in islets isolated from control, $\beta\text{Insr}^{\text{HET}}$, $\beta\text{Insr}^{\text{KO}}$ female (n=7,5,6) and male (n=5,4,3) mice. Data were analyzed by 1-way ANOVA. **(M,N)** Insulin content of 10 islets isolated from control, $\beta\text{Insr}^{\text{HET}}$, $\beta\text{Insr}^{\text{KO}}$ female (n=4,3,5) and male (n=5,4,5) mice. Data were analyzed by 1-way ANOVA.

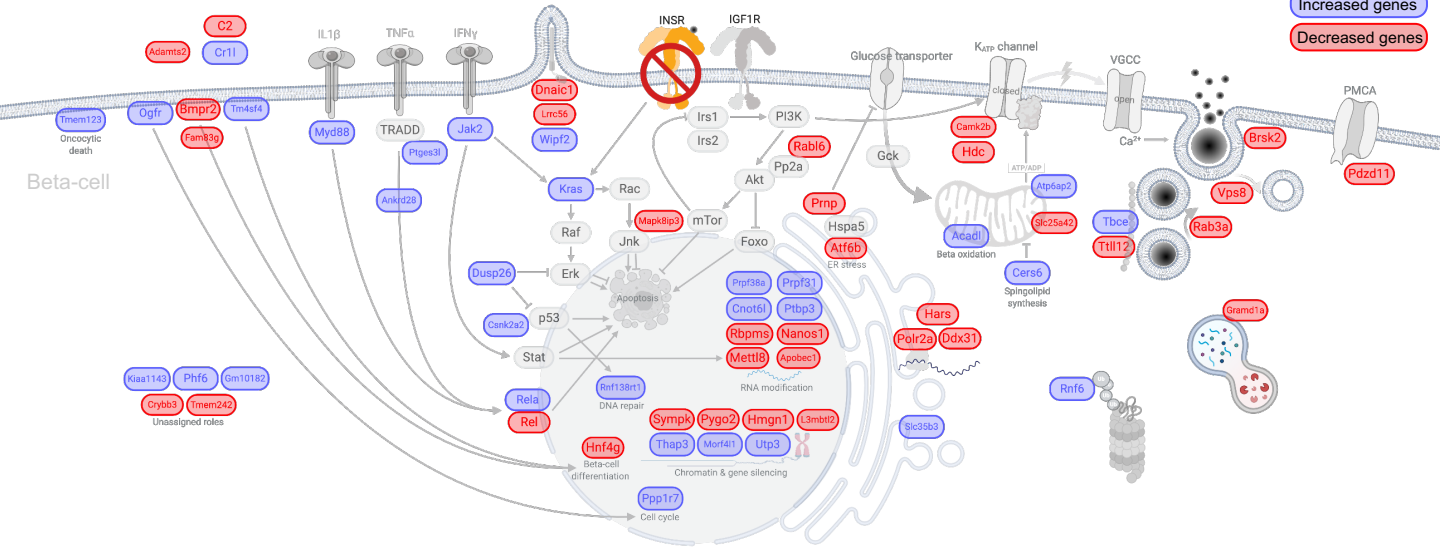
Figure 5. Islet cell proliferation and relative area in mice lacking β -cell *Insr*. **(A)** A representative image showing islet architecture via staining for insulin, glucagon and DNA. **(B-E)** β -Cell area shown as a percentage of total pancreatic area. Data were analyzed by 1-way ANOVA analyses. **(F-S)** 4-day *in vivo* glucose infusion in female (n=5 control, 4 $\beta\text{Insr}^{\text{KO}}$) and male (n=6 control, 8 $\beta\text{Insr}^{\text{KO}}$) mice. **(F,M)** Tail blood glucose and **(G,N)** insulin data were analyzed using repeated measures mixed effects model. **(H,O)** 4 day average plasma insulin data were analyzed by an unpaired t-test. **(I,P)** Plasma glucagon (tail blood) data were analyzed using repeated measures mixed effects model. **(J,Q)** 4 day average plasma insulin data were analyzed by an unpaired t-test. **(K,R)** Representative single channel and merge images showing islets stained for insulin, glucagon, BrdU and DNA from LFD-fed female and male controls and female $\beta\text{Insr}^{\text{KO}}$ and male $\beta\text{Insr}^{\text{KO}}$ mice following 4day glucose infusion. **(L,S)** Quantification of BrdU+ insulin+ cells and . BrdU+ glucagon+ cells. Data were analyzed by an unpaired t-tests. **(T)** Representative western blot image and quantification of islet lysate from male $\text{Insr}^{\text{wt/wt}}, \text{Ins}^{\text{cre/wt}}, \text{nTnG}$ (black bar, n=3), $\text{Insr}^{\text{f/f}}, \text{Ins}^{\text{cre/wt}}, \text{nTnG}$ (light blue bar, n=3), $\text{Insr}^{\text{f/f}}, \text{Ins}^{\text{1cre/wt}}, \text{nTnG}$ (dark blue bar, n=3) mice treated with 3 mM or 20 mM glucose. Data were analyzed by 1-way ANOVA.

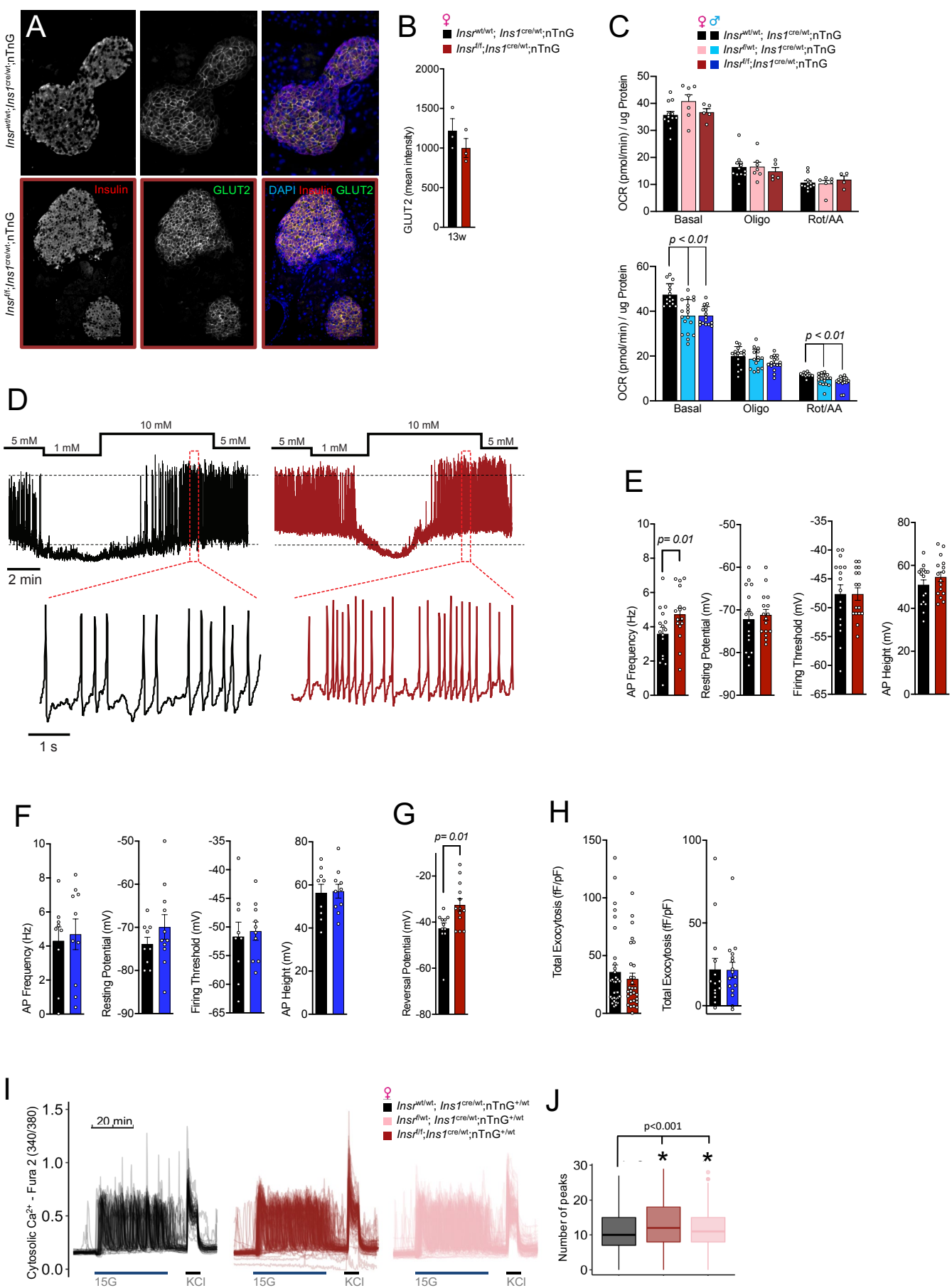
Figure 6. Glucose tolerance at multiple ages in β -cell specific *Insr* knockout mice fed 2 different diets. **(A)** modified version of the Topp model. **(B, C)** Simulations of the effects of reduced β -cell insulin sensitivity on glucose stimulated insulin release and glucose tolerance. **(D, E)** Relationship between the contributes of peripheral insulin sensitivity and β -cell insulin sensitivity to the glucose AUC and insulin AUC in the *in silico* glucose tolerance tests. **(F)** Glucose tolerance tests of control, $\beta\text{Insr}^{\text{HET}}$, $\beta\text{Insr}^{\text{KO}}$ LFD-fed female (n_{4week}=16,16,14; n_{9week}=23,25,17; n_{21week}=12,15,12; n_{39week}=8,12,10) and male (n_{4week}=10,18,5; n_{9week}=17,30,11; n_{21week}=8,14,8; n_{39week}=9,7,13) as well as HFD-fed female (n_{9week}=17,17,14; n_{21week}=12,14,12 n_{39week}=14,16,10; n_{54week}=10,13,11) and male (n_{9week}=7,16,9; n_{21week}=7,16,8; n_{39week}=8,14,8; n_{54week}=6,11,7) mice. (All mice received a glucose bolus of 2g glucose/kg body mass (*i.p.*) except older HFD-fed males, which received only 2g glucose/kg body mass (*i.p.*). **p*-values are italicized when $\beta\text{Insr}^{\text{KO}}$ was compared to controls, p-values are underlined when $\beta\text{Insr}^{\text{HET}}$ was compared to controls. **(G)**. The glucose tolerance of Chow-fed $\text{Insr}^{\text{wt/wt}}, \text{MIP}^{\text{Cre-ERTM}}, \text{YFP}^{+/+}$ (n=7) and $\text{Insr}^{\text{f/f}}, \text{MIP}^{\text{Cre-ERTM}}, \text{YFP}^{+/+}$ (n=17) mice were examined at 4, 8, 16 and 20 weeks after tamoxifen injection (8 weeks of age upon tamoxifen injection (3 x 200 mg/kg over a 1-week period). Data were analysed using repeated measures mixed effects models.

Figure 7. Effects of β -cell specific *Insr* deletion fasting glucose, body weight and organ weight. **(A-D)** Plasma glucose concentration after a 4-h fast in control, $\beta\text{Insr}^{\text{HET}}$, and $\beta\text{Insr}^{\text{KO}}$ mice at multiple ages in both LFD and HFD. **(E-H)** Longitudinally tracked body weight in control, $\beta\text{Insr}^{\text{HET}}$, and $\beta\text{Insr}^{\text{KO}}$ mice at multiple ages in both LFD and HFD. **(I,J)** Weights, as a percentage of the whole body, of inguinal adipose tissue, gonadal adipose tissue, liver, brown adipose tissue and skeletal muscle. Data were analysed using repeated measures mixed effects models. **(K)** Representative immunoblot of *Insr* (n = 4).

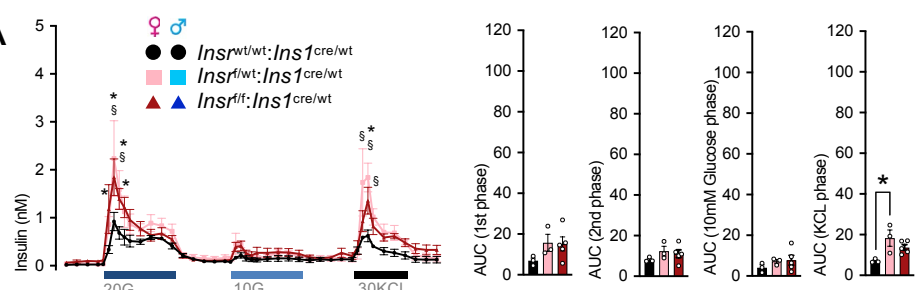


Increased genes
Decreased genes

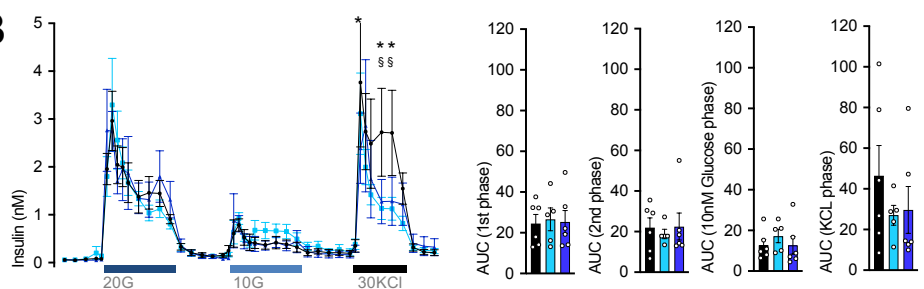




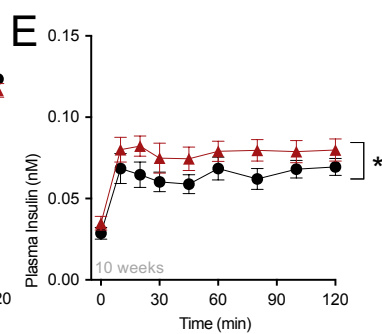
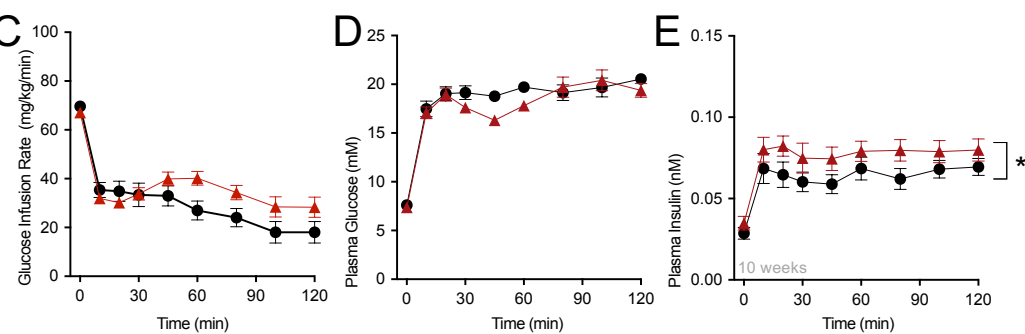
A



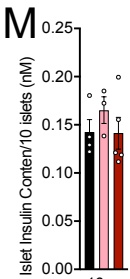
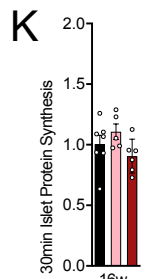
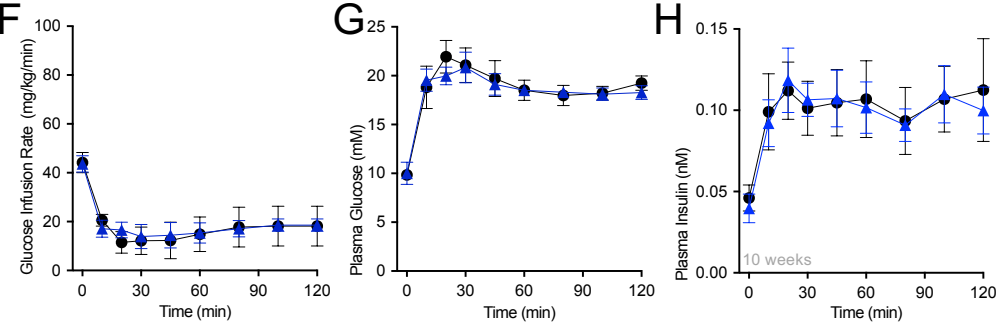
B



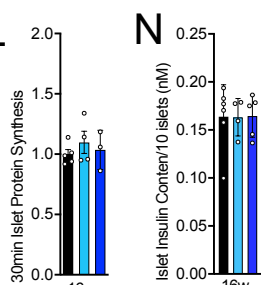
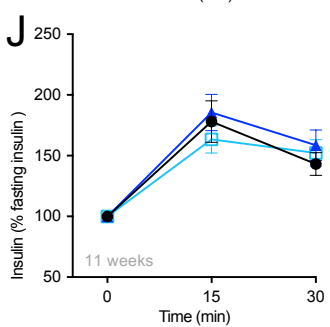
C



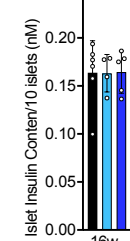
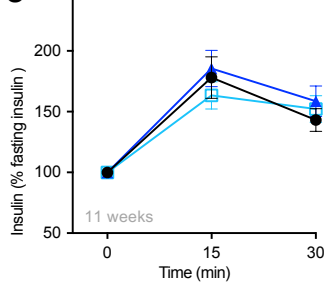
F

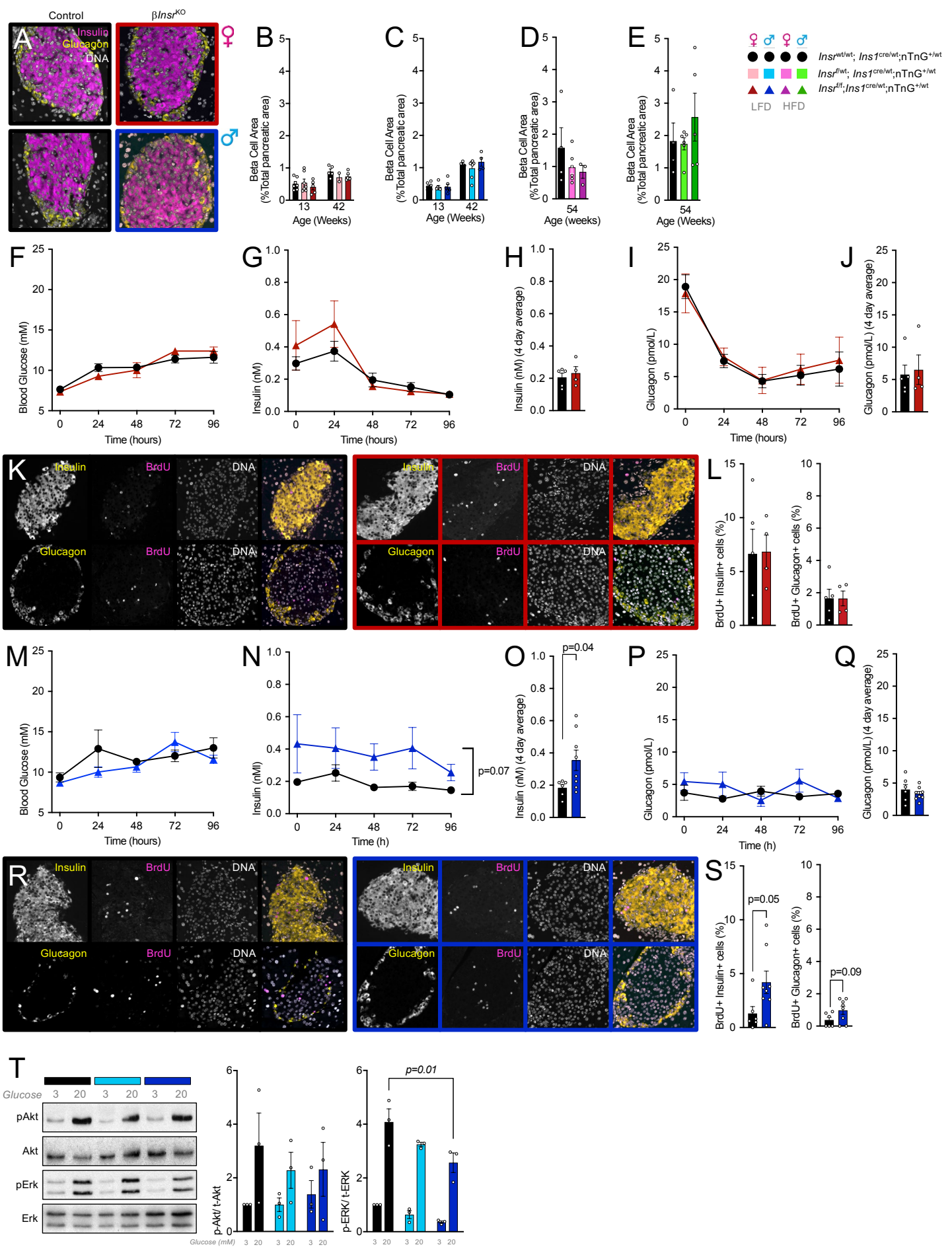


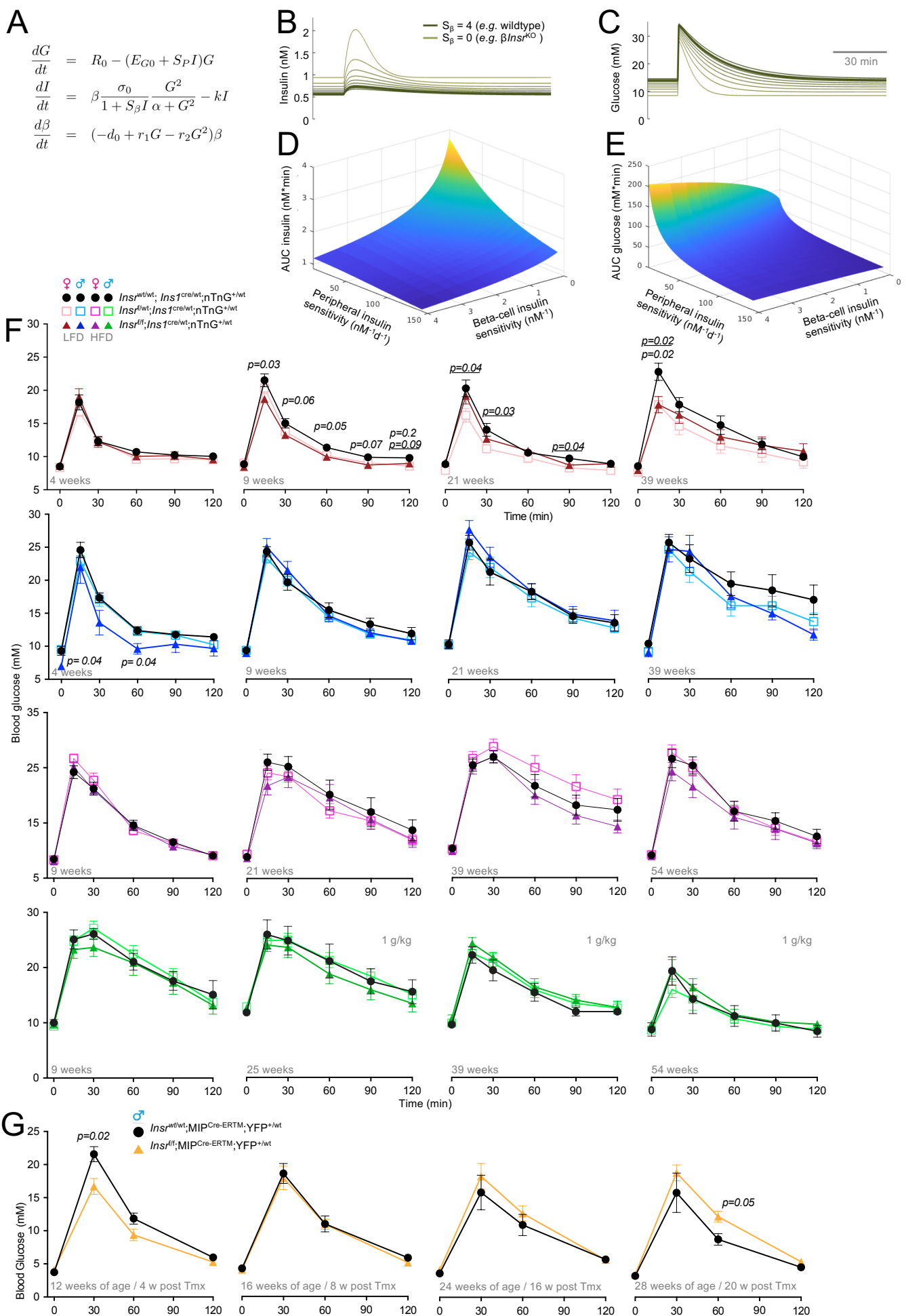
J

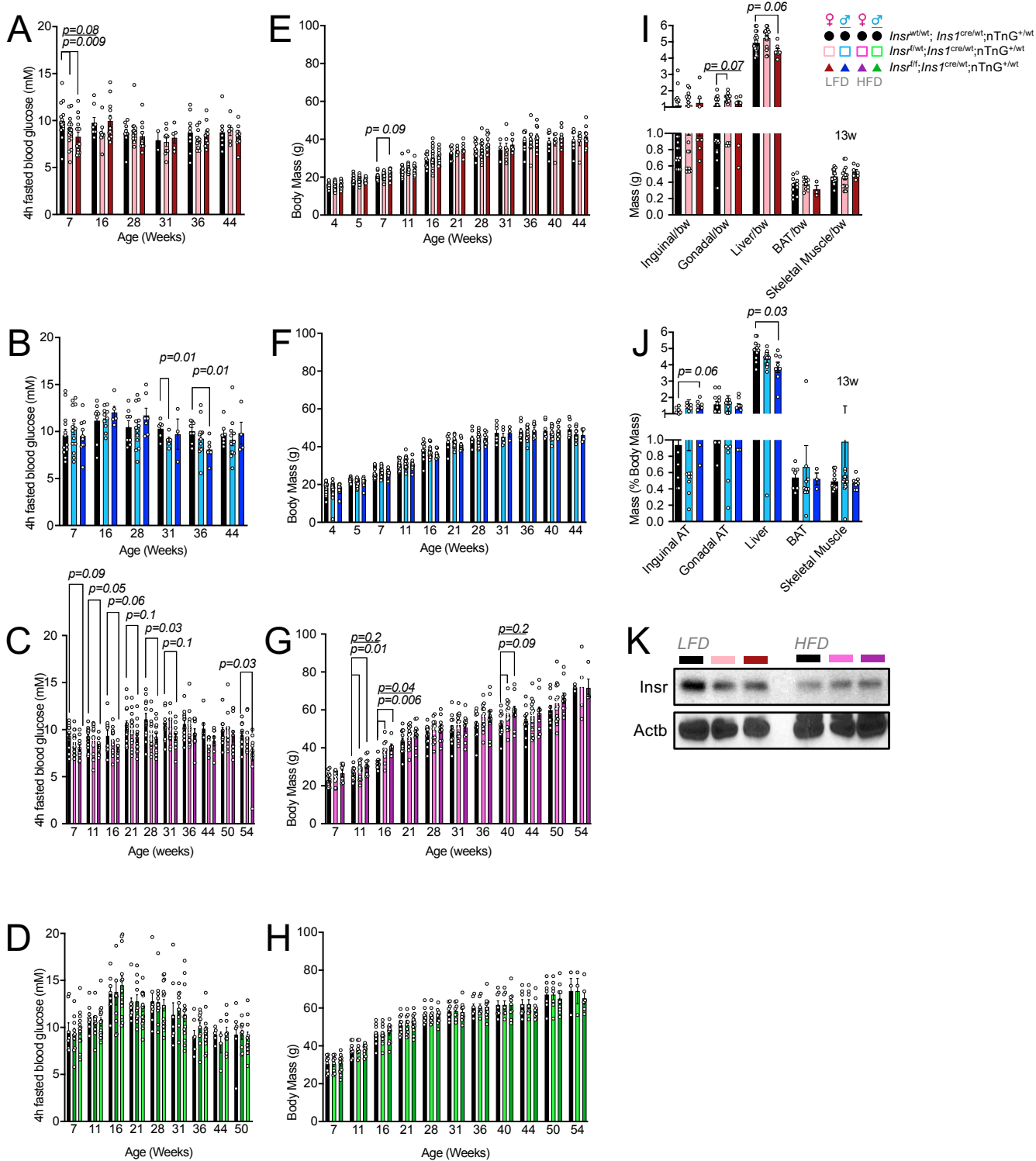


L









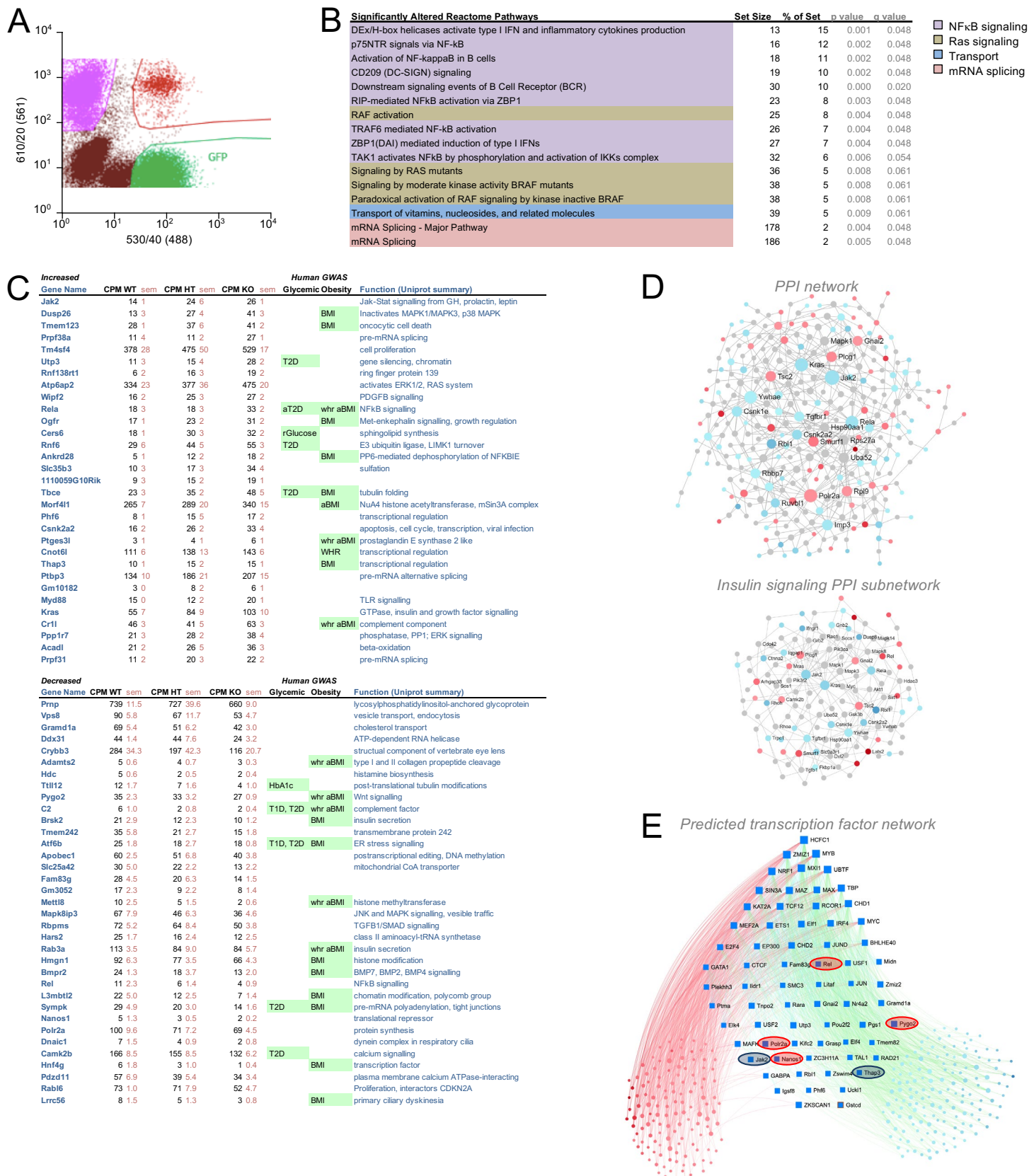


Fig. S1. RNA sequencing analysis of Insr-deficient purified beta-cells. (A) FACS plot example of sorted cells. (B) Significantly different Reactome Pathways. (C) List of most significantly upregulated or downregulated individual genes. Data are shown for control control, $\beta/Insr^{HET}$, and $\beta/Insr^{KO}$ ($n=4-7$). (D) Protein-protein interaction networks constructed around differentially expressed genes. (E) Transcription factors predicted to mediated differential gene expression. Individual transcription factors that were increase (blue) or decreased (red) are highlighted.

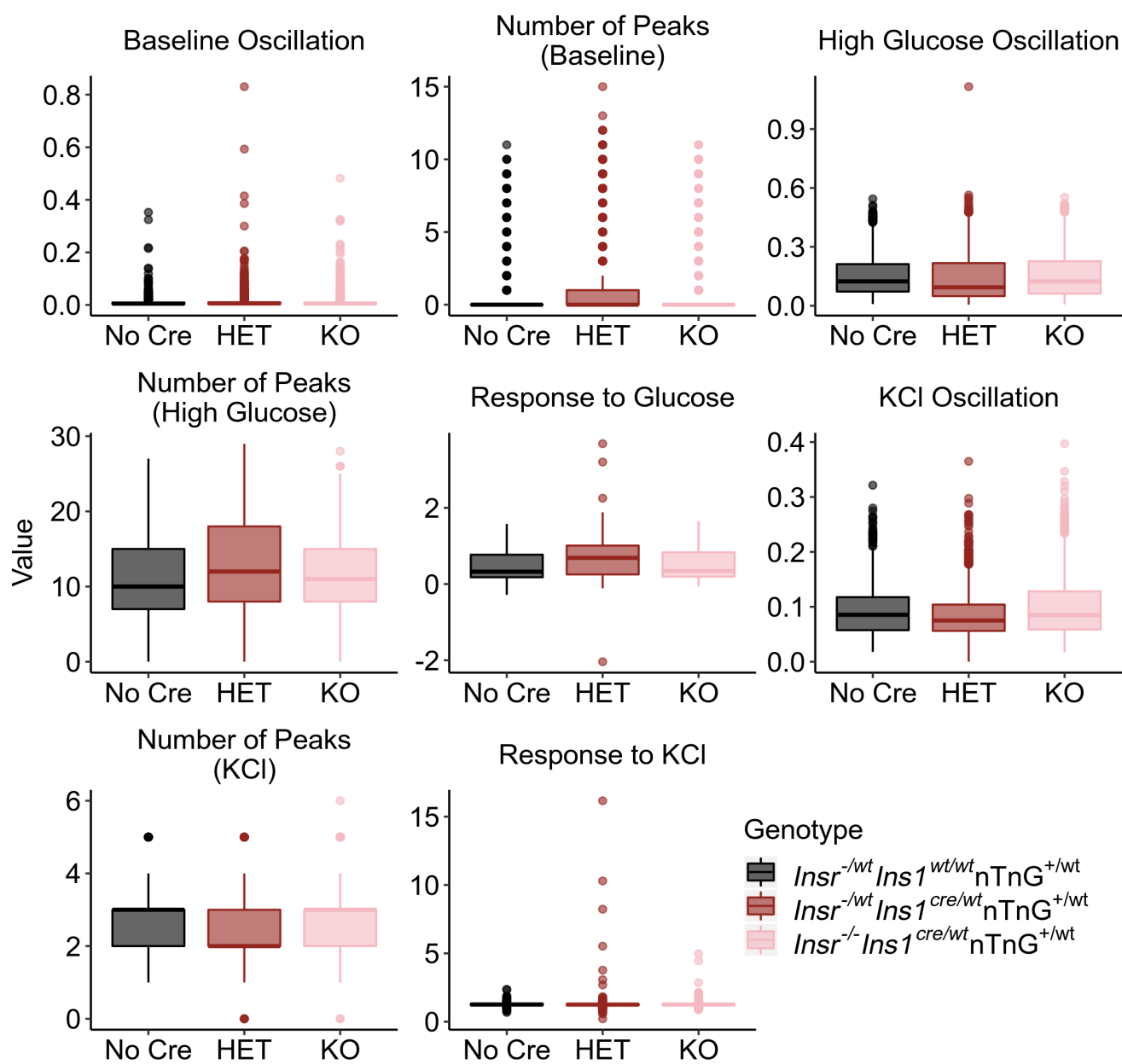


Fig. S2. Additional quantification of dynamic Ca^{2+} responses. Responses to glucose or KCl were defined as the median high glucose (15mM) or KCl (30mM) signal above baseline glucose (3mM), respectively, and normalized to the maximum response to KCl above baseline. High glucose-stimulated Ca^{2+} oscillations, Ca^{2+} oscillation in low glucose, and KCl-stimulated Ca^{2+} oscillation were defined as the median absolute deviation (MAD) during the high glucose, low glucose or KCl exposures, respectively, normalized to the maximum response to KCl above baseline.

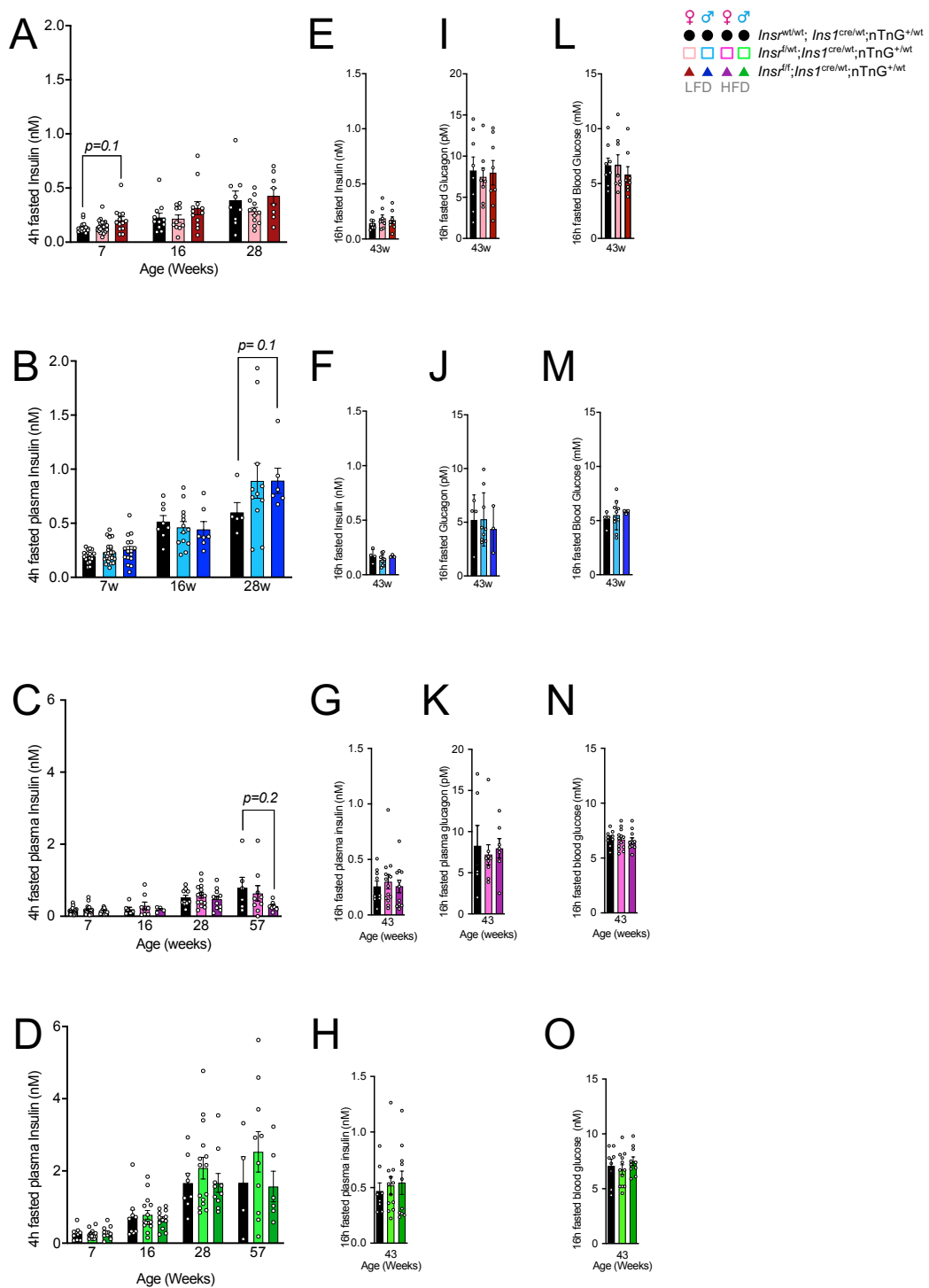


Fig. S3. Fasting insulin, glucagon, and glucose levels. **(A-D)** Circulating plasma insulin levels after a 4-hour fast, **(E-H)** or a 16-hour fast; **(I-K)** plasma glucagon levels after a 16-hour fast **(L-O)** plasma glucose concentration after a 16-hour fast in control, β /Insr^{HET}, and β /Insr^{KO} mice at multiple ages.

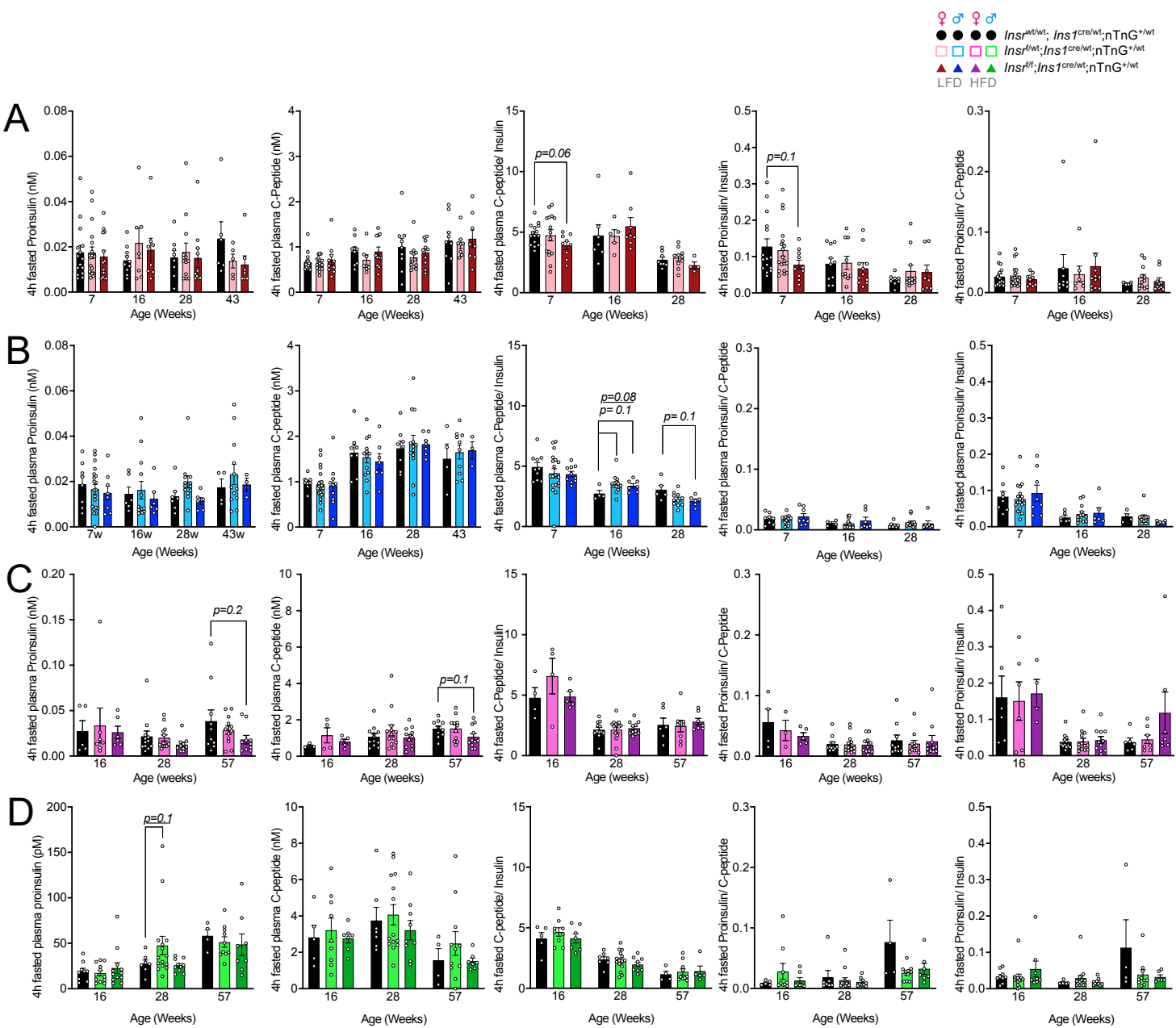


Fig. S4. Fasting proinsulin and C-peptide. (A-D) Circulating plasma proinsulin and C-peptide levels after a 4-hour fast, and their associated ratios in control, $\beta/\text{Ins}^{\text{HET}}$, and $\beta/\text{Ins}^{\text{KO}}$ mice at multiple ages. Statistical analyses were done with a mixed model.

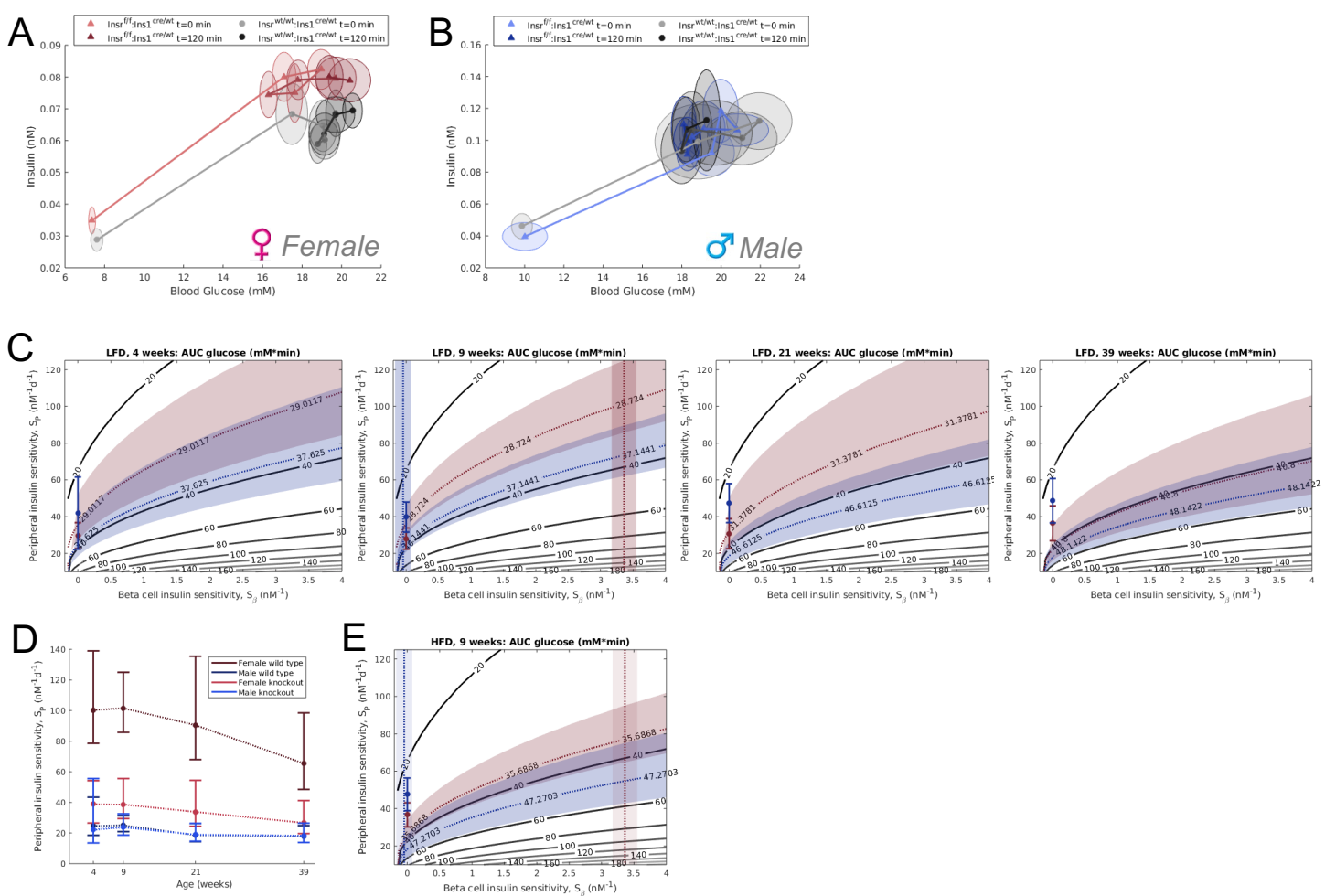


Fig. S5 Mathematical modeling of glucose tolerance. **(A,B)** Relationship between insulin and glucose during the hyperglycemia clamps over time in female and male mice. Data from the clamp studies were used to define a beta-cell insulin sensitivity term that was included in a modified Topp model (see main text). **(C)** Modelled effects of peripheral insulin sensitivity and beta-cell insulin sensitivity on glucose AUC (topographical lines). Female response is shown in the pink shadow and male response in the blue shadow. The experimental effects of the knockout are shown as the single data point with SEM bars. **(D)** Model-assessed change in peripheral insulin sensitivity with age, using experimental data. **(E)** Effects of HFD at 9 weeks, where comparable glucose bolus was given.

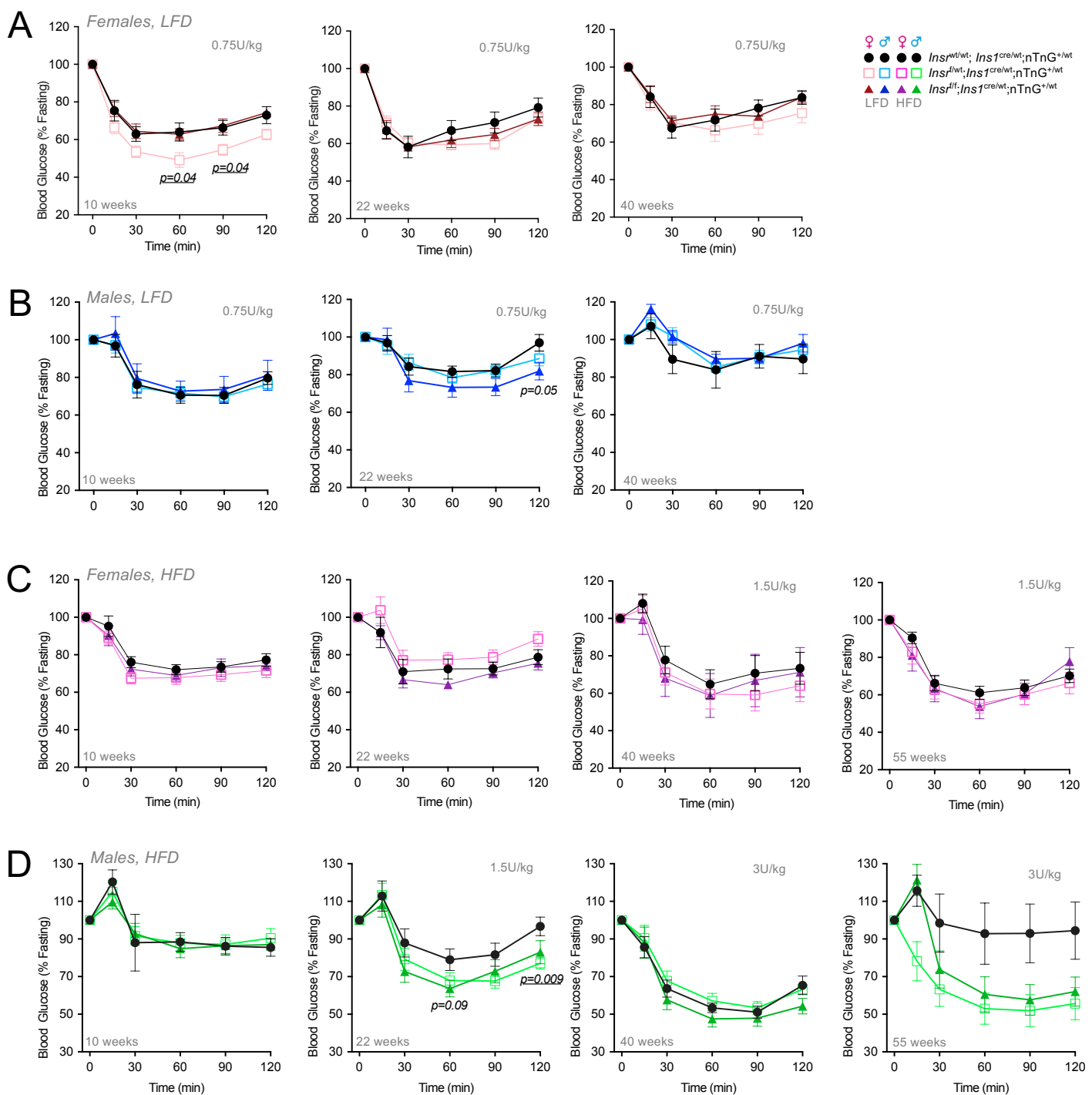


Fig. S6. Insulin tolerance tests. (A-D) Insulin tolerance tests after a 6 hour fast in control, $\beta/Insr^{HET}$ and $\beta/Insr^{KO}$ mice fed LFD or HFD at multiple ages (n=5-26). Statistical analyses were done with repeated measures 2-way ANOVA. Doses are 0.75 U/kg unless otherwise shown.

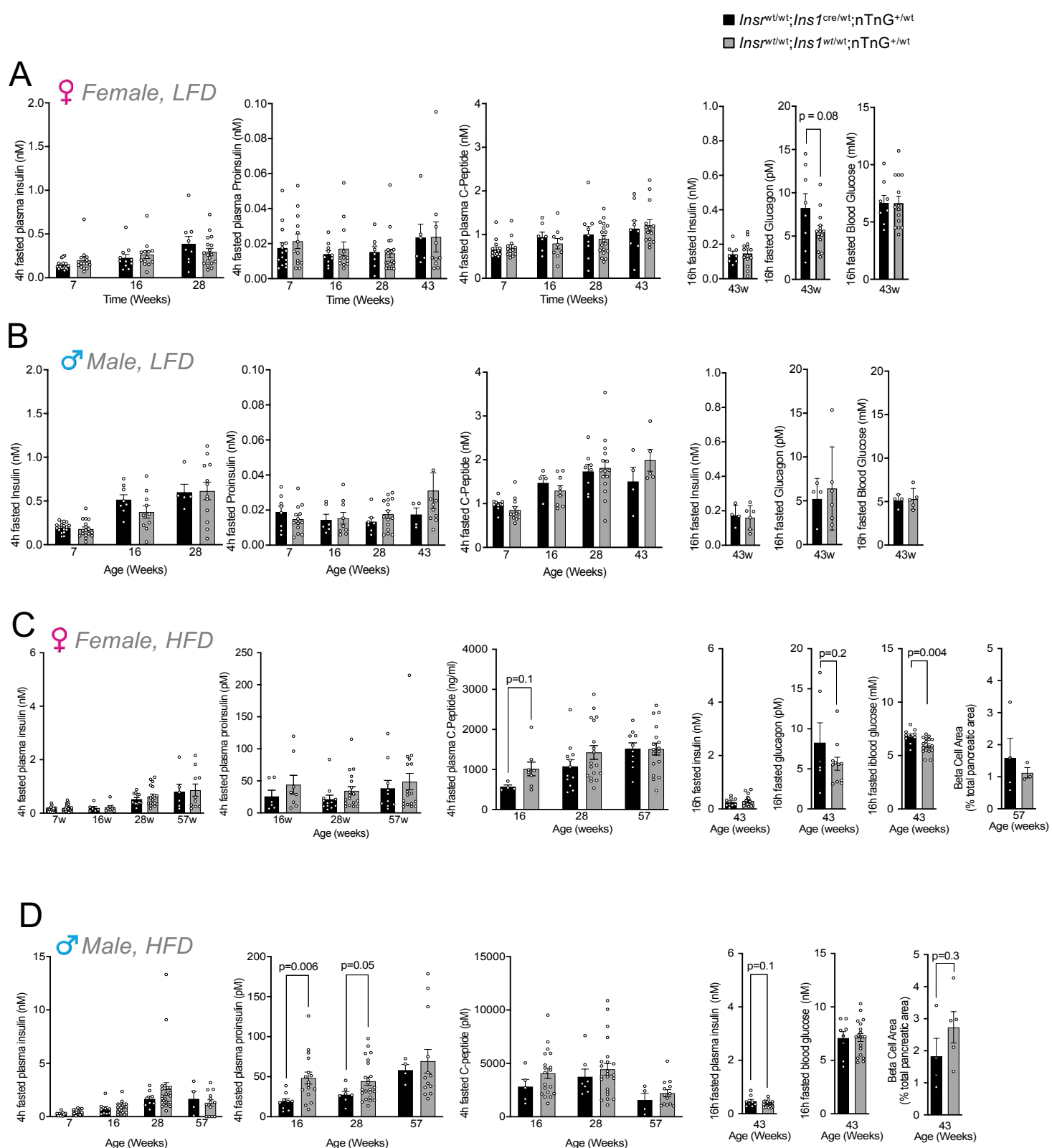


Fig. S7. Fasting insulin, proinsulin, C-peptide and glucagon in control mice. (A-D) Circulating plasma insulin, proinsulin and C-peptide levels after a 4-hour fast, and their associated ratios as well as 16-hour fasted insulin, glucagon and blood glucose levels in *Insr^{wt/wt};Ins1^{Cre/wt};nTnG^{+/-}* (black) and *Insr^{wt/wt};Ins1^{wt/wt};nTnG^{+/-}* (grey) LFD-mice at multiple ages.

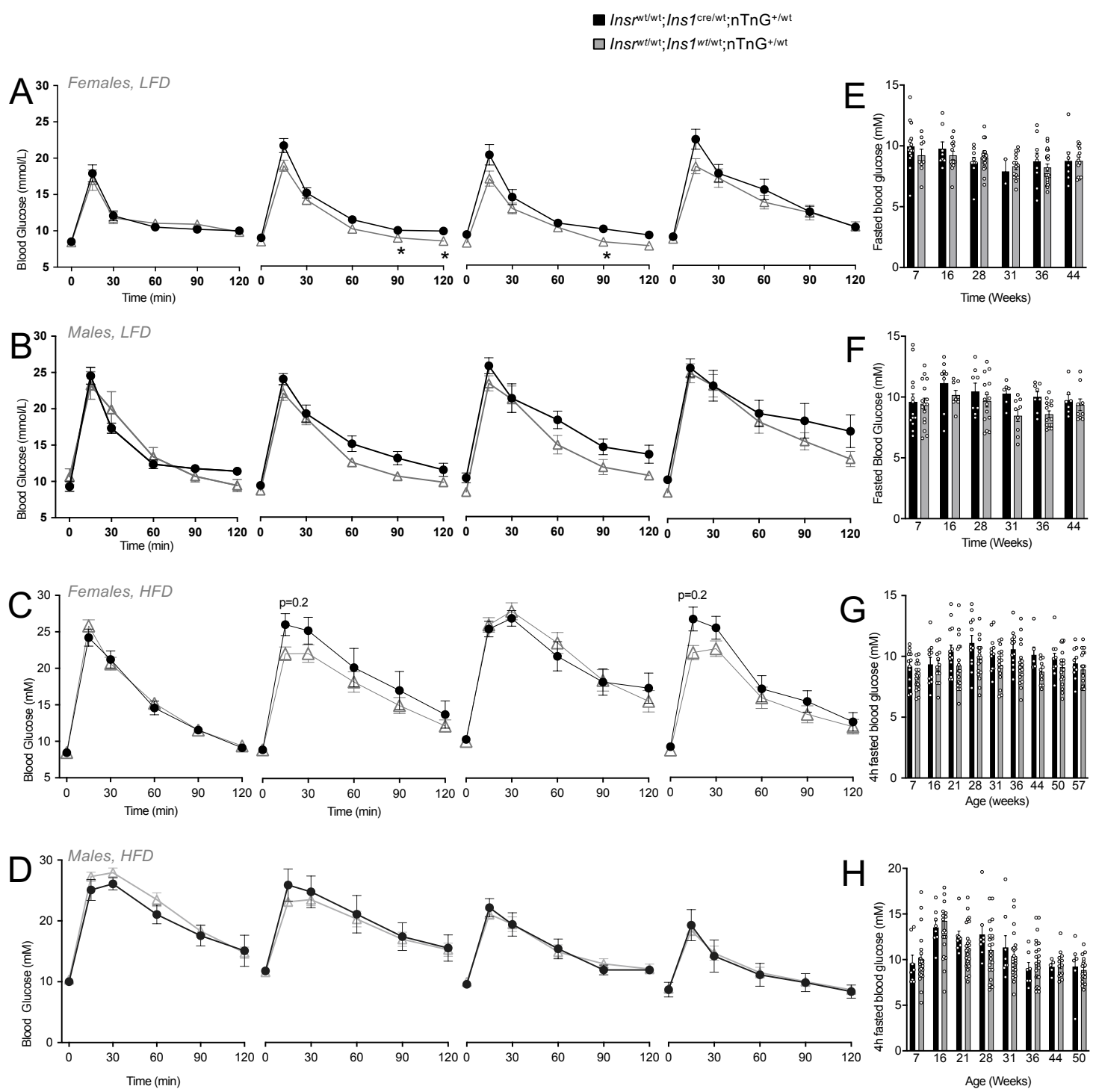


Fig. S9. Glucose tolerance and fasting glucose comparison in controls. (A-D) Glucose tolerance tests after a 6 hour fast in female and male of $Insr^{wt/wt}; Ins1^{Cre/wt}; nTnG^{+/wt}$ (black) and $Insr^{wt/wt}; Ins1^{wt/wt}; nTnG^{+/wt}$ (grey) fed LFD or HFD at multiple ages (n=5-30). Statistical analyses were done with repeated measures 2-way ANOVA. (E-H) Blood glucose after a 4 hour fast.

■ $Insr^{wt/wt};Ins1^{Cre/wt};nTnG^{+/wt}$
 □ $Insr^{wt/wt};Ins1^{wt/wt};nTnG^{+/wt}$

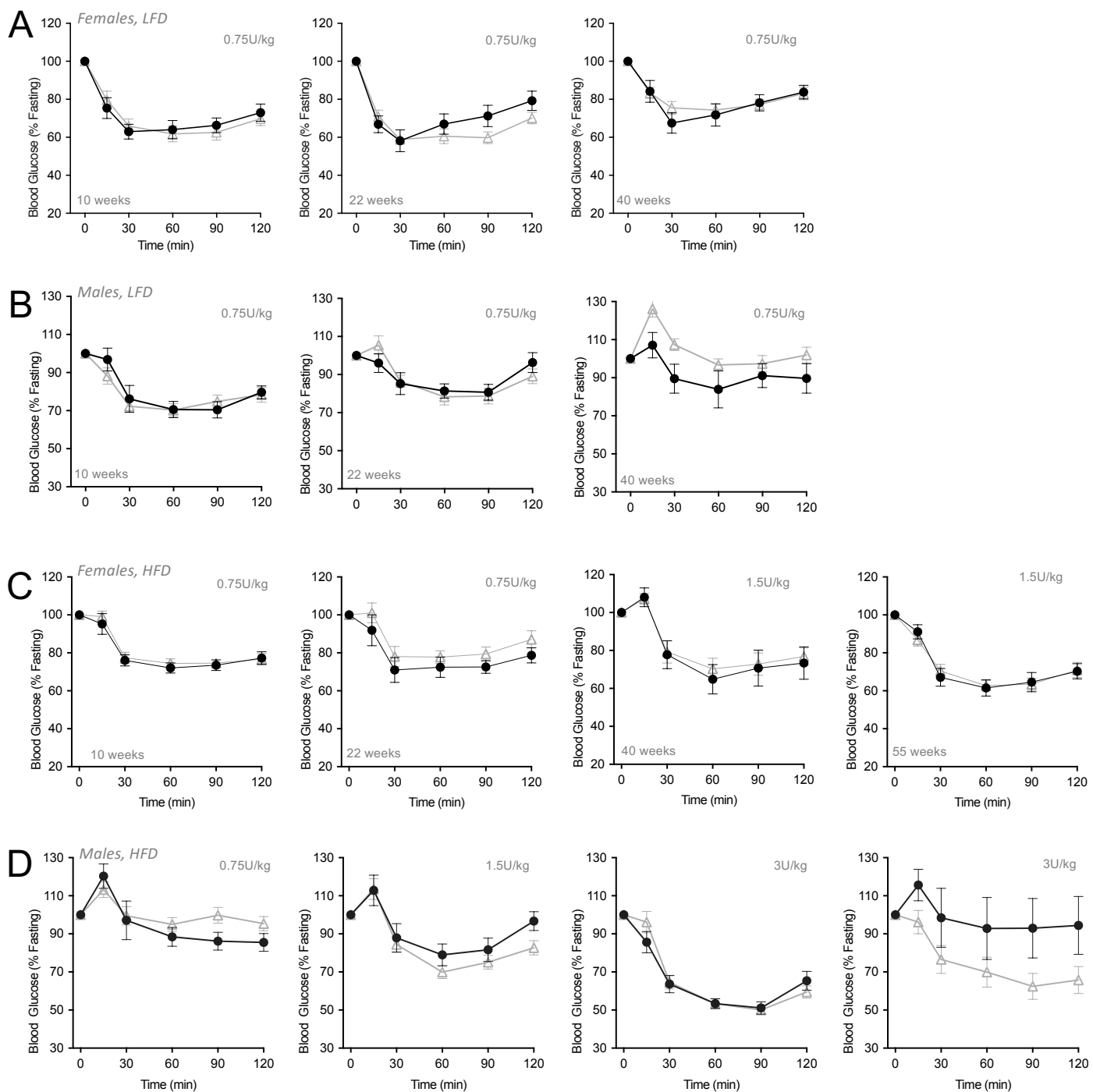


Fig. S9. Insulin tolerance tests in control mice. (A-D) Insulin tolerance after a 6 hour fast in female and male of $Insr^{wt/wt};Ins1^{Cre/wt};nTnG^{+/wt}$ (black) and $Insr^{wt/wt};Ins1^{wt/wt};nTnG^{+/wt}$ (grey) fed LFD or HFD at multiple ages (n=5-30). Statistical analysis were done with repeated measures 2-way ANOVA. Doses are 0.75 U/kg unless otherwise shown.

■ *Insr^{wt/wt};Ins1^{Cre/wt};nTnG^{+/wt}*
 □ *Insr^{wt/wt};Ins1^{wt/wt};nTnG^{+/wt}*

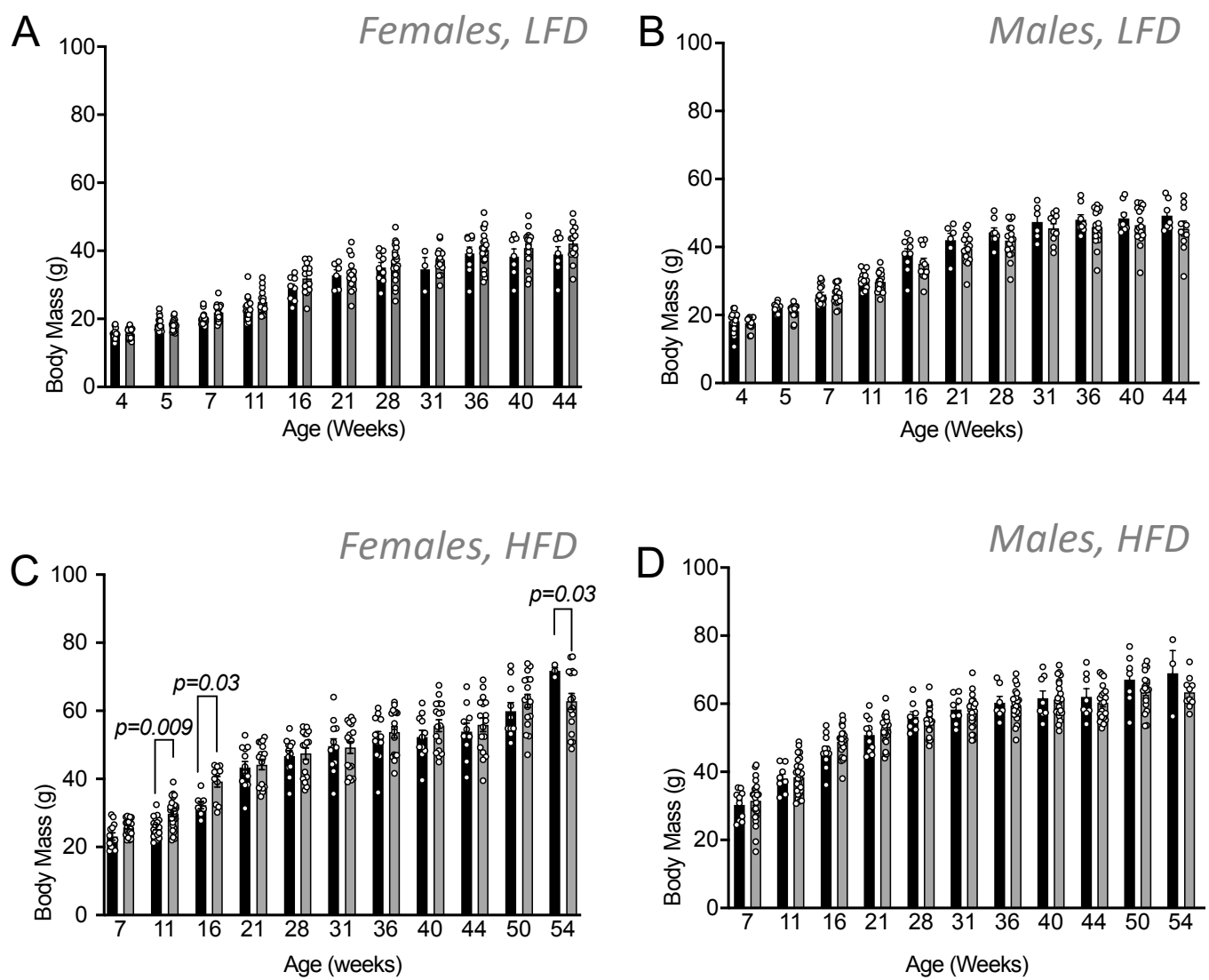


Fig. S10. Body weight in control mice. (A-D) Body weight in female and male of *Insr^{wt/wt};Ins1^{Cre/wt};nTnG^{+/wt}* (black) and *Insr^{wt/wt};Ins1^{wt/wt};nTnG^{+/wt}* (grey) fed LFD or HFD at multiple ages. Statistical analysis with mixed effect model.